Engineering Geology 332 (2024) 107474

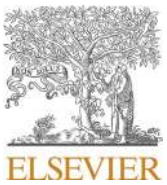

Contents lists available at ScienceDirect

Engineering Geology

journal homepage: www.elsevier.com/locate/enggeo

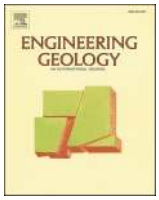

National-scale assessment of railways exposure to rapid flow-like landslides

Ivan Marchesini [a,*], Omar Althuwaynee [a], Michele Santangelo [a], Massimiliano Alvioli [a], Mauro Cardinali [a], Martin Mergili [b], Paola Reichenbach [a], Silvia Peruccacci [a], Vinicio Balducci [a], Ivan Agostino [c], Rosaria Esposito [c], Mauro Rossi [a]

[a] National research Council, Research Institute for Geo-Hydrological protection (CNR IRPI), Perugia, Italy
[b] University of Graz, Institute of Geography and Regional Science, Graz, Austria
[c] Technical Department, Rete Ferroviaria Italiana S.P.A, Rome, Italy

ARTICLE INFO

Keywords:
Flow-like landslides
Railway
Debris flow
Susceptibility
Exposure
Italy

ABSTRACT

In landslide-prone regions, railway networks are vulnerable to rapid flow-like landslides, which can cause extensive damage, even at significant distances from the landslide's point of origin. The prioritization of protective measures on a national scale depends on the accurate assessment of each railway segment's exposure to landslides.

This study introduces a methodology for evaluating the exposure of transportation infrastructure, with a specific focus on flow-like landslides. The application of this methodology is demonstrated on Italy's national railway network.

The methodology involves a multi-phase approach, including a training phase using DEM data and landslide inventories, a modeling phase for landslide source areas and runout, and a final phase for infrastructure exposure assessment. Key outputs of this approach include the creation of a landslide susceptibility map and, critically, the generation of an exposure map that quantifies the risk to transportation infrastructure posed by flow-like landslides.

Validation using an independent landslide dataset demonstrated satisfactory results, especially in regions with area under the ROC curve values ranging from 0.7 to 0.95. The resulting exposure map shows that approximately 13.4% (2376 km) of the entire national railway network is exposed to a medium-high level of risk from flow-like landslides.

This methodology highlights its effectiveness in nationwide exposure analysis of transportation infrastructure, providing valuable insights for risk mitigation and resource allocation, while relying solely on existing landslide inventories and digital elevation models.

1. Introduction

Landslides represent a prevalent natural hazard impacting transportation infrastructures, encompassing both railways (Liu et al., 2018; Zhao et al., 2020) and roads (Jaiswal et al., 2010), (Bornaetxea et al., 2022; Tanyaş et al., 2022; Taylor et al., 2020). Diverse slope movements are capable of inflicting direct harm upon railways, and in particular to tracks, vehicles, and individuals in transit (Laimer, 2017; Martinović et al., 2016). Assessing the exposure of linear infrastructures to landslides is of paramount importance for network management, even on a large scale (Firmi et al., 2021; Samela et al., 2023), also considering that railways exposure is projected to rise due to climate change impacts (Schlögl and Matulla, 2018). In this paper, we focus on rail networks and consider "exposed" transportation infrastructure that lies within the landslide runout path (Corominas et al., 2014; He et al., 2023; Luo et al., 2023).

Exposure in transportation systems pertains to their susceptibility to damage or disruption caused by hazards like natural disasters and climate change. It can be evaluated by considering factors like infrastructure location, design, construction, and protective measures (Petrova and Bostenaru Dan, 2020). In Italy, Firmi et al. (2021) estimated that approximately 7700 km or approximately 45% of railway routes are susceptible to various landslide types. In the UK, around 36% of the national railway network is located in regions where slope instability

* Corresponding author.
E-mail address: ivan.marchesini@irpi.cnr.it (I. Marchesini).

https://doi.org/10.1016/j.enggeo.2024.107474
Received 2 November 2023; Received in revised form 6 March 2024; Accepted 7 March 2024
Available online 11 March 2024

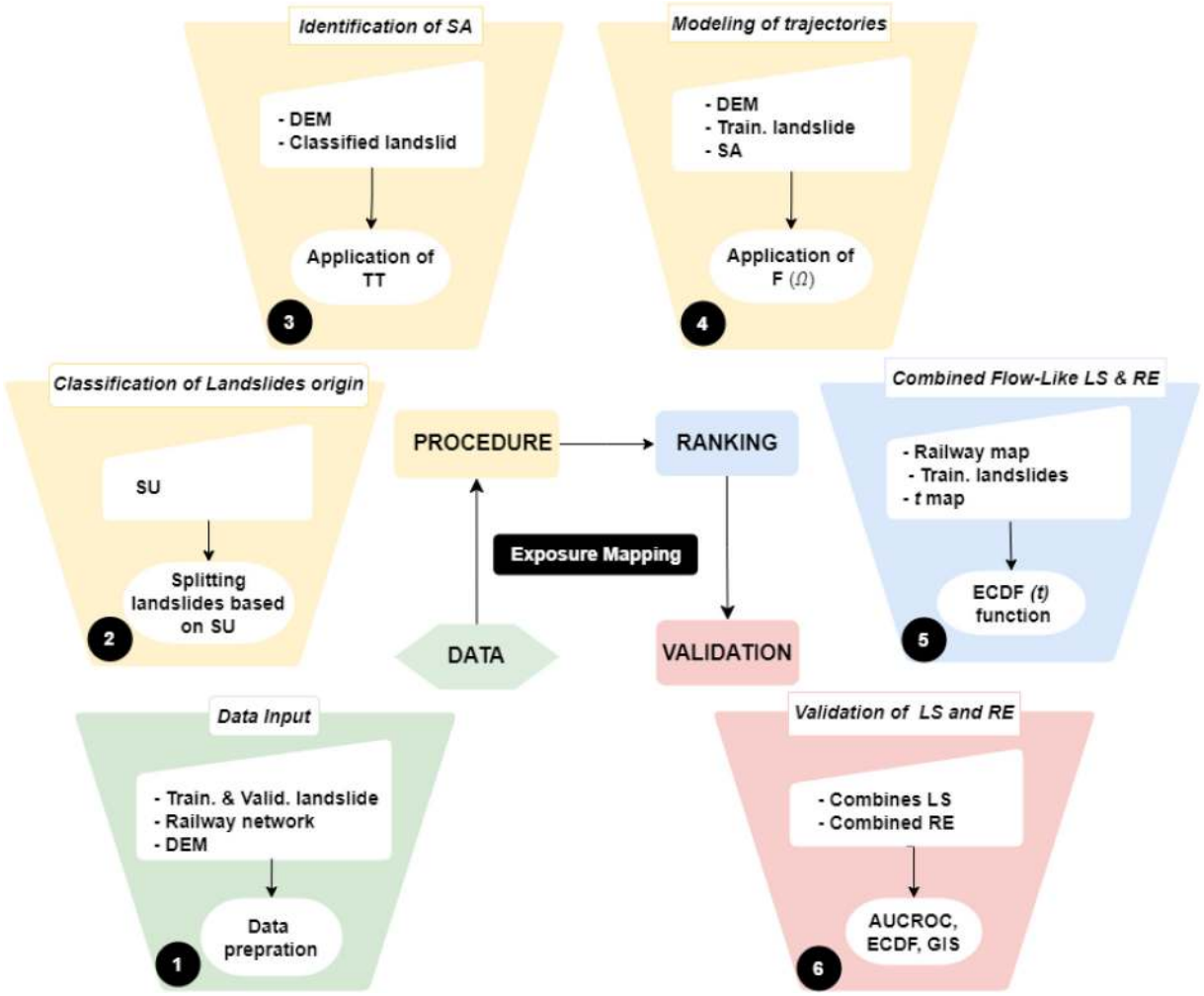

Fig. 1. Flowchart of the methodology for assessing the exposure of a network transportation infrastructure to rapid flow-like landslides. SA (source area - §2.2); SU (slope unit - §2.1); TT (Topographic Threshold - §2.2), $F(\Omega)$ (statistic distribution of reach angle values - §2.3), t map (map of number of random walks paths - §2.3), ECDF (empirical cumulative distribution function - §2.4 and §2.5), LS (landside susceptibility - §2.4), RE (Railway Exposure - §2.4), AUROC (area under the ROC curve - §2.5).

issues may be present or anticipated (Freeborough et al., 2016).

The specific manifestations of landslides affecting railways are contingent upon geological and geomorphological settings (Laimer, 2017; Lan et al., 2008; Martinović et al., 2016) and the presence and maintenance levels of engineered slopes (Voumard et al., 2018). These events encompass different types of landslides types (Voumard et al., 2018). Among these, debris flows, mudflows and debris avalanche movements (in this paper "rapid flow-like landslides", partially exploiting the Hungr et al. (2014) classification) can be extremely dangerous and damaging to railways because their propagation speed and distance assume a critical role in their destructive potential. Rapid flow-like landslides, particularly debris flows, may be classified into channelized and hillslope phenomena (Chen et al., 2009; Lorente et al., 2003; Zhang et al., 2013), based on disparities in triggering mechanisms, affected areas, and primarily, runout lengths.

Several methods and approaches, predominantly rooted in statistical and machine learning techniques, have been proposed to evaluate the exposure of railway networks to landslides at the national scale (e.g., (Freeborough et al., 2018; Freeborough et al., 2016; Liu et al., 2018; Yin et al., 2022; Zhao et al., 2020). However, many of these approaches focus primarily on the classification of study areas in terms of susceptibility to landslide occurrence, while not taking into account runout (which for flow-like landslides can be very relevant) and their possible interaction with transport infrastructure.

Spatial probability of landslides triggering (susceptibility) can be evaluated using distributed physically-based modeling (e.g. (Alvioli et al., 2021, 2023; Bozzolan et al., 2023; Cabral et al., 2023; Mergili et al., 2018; Mergili et al., 2014a; Mergili et al., 2014b; Reichenbach et al., 2018; Van den Bout et al., 2022). However those models are demanding in terms of input data quality and quantity, and this requirement remains a challenge over large areas (Gariano and Guzzetti, 2016; Marin et al., 2021; Palacio Cordoba et al., 2020; Park et al., 2019), also because detailed information on geotechnical characteristics of soil/subsoil is rarely available and hard to spatialize (de Lima Neves Seefelder et al., 2017; Mergili et al., 2018) Conversely data-driven models impose fewer data requirements and offer a robust alternative for modeling susceptibility to landslide occurrence over vast territories, from the local to the global scale (e.g. (Carrara et al., 2008; Felsberg et al., 2022; Jia et al., 2021; L. Lin et al., 2017; Q. Lin et al., 2021; Loche et al., 2022).

For simulating landslide runout paths, physically-based approaches can be replaced by the conceptual models, which exploit empirical laws and terrain elevation data (Horton et al., 2013; Liang et al., 2023; Mergili et al., 2015, 2019; Steger et al., 2022), and that, to the best of our knowledge, have never been used for modeling, separately, hillslope and channelized rapid flow-like landslides, at least at national scale.

To date, no comprehensive research studies exist in Italy, or to our knowledge, in any other major nation, aiming to assess the exposure of

Table 1
Scheme used to classify the relative probability of each raster cell to be a source area of rapid flow-like failure (S_A is the slope value of a cell with a flow accumulation area A).

Conditions	Source area relative probability
$\beta_{05}(A) \leq S_A < \beta_{10}(A)$	5%
$\beta_{10}(A) \leq S_A < \beta_{25}(A)$	15%
$\beta_{25}(A) \leq S_A < \beta_{75}(A)$	50%
$\beta_{75}(A) \leq S_A < \beta_{90}(A)$	15%
$\beta_{90}(A) \leq S_A \leq \beta_{95}(A)$	5%

entire rail networks to flow-like landslides at the national scale. Such studies should ideally incorporate (i) a fusion of statistical and conceptual models for source area and runout characterization, (ii) the separate consideration of hillslope and channelized phenomena, (iii) quantitative assessment of the exposure of the railway network and (iii) rigorous validation employing datasets distinct from and more extensive than those used for model training.

Within Italian territory, at least two recent studies have explored the impact of landslides on railway infrastructure. The first study, conducted by Alvioli et al. (2021), covered the entirety of the Italian railway network but did not address flow-like landslides. Instead, it assessed the exposure of the main national railway network to rockfall phenomena. More recently, Samela et al. (2023) introduced a methodological framework for evaluating flood hazards along land transport infrastructures at a national scale. While this framework considered potential interactions between infrastructure and debris flows, it was primarily applied to a limited selection of medium-sized hydrological basins in Italy.

In this paper we propose, describe and apply, over the entire Italian railway network, a procedure that relies solely on landslide inventories and topographic data to (i) assess susceptibility to hillslope and channelized rapid flow-like landslides and (ii) rank the exposure levels of transportation routes and network segments to these specific phenomena. The paper is organized as follows: Section (§) 2 outlines the general methods, including modeling approaches, exposure analysis, and the validation scheme; §3 delineates the case study of the Italian railway network and the landslide data used for modeling and validation. §4 presents, validates and discusses the results. §5 provides a summary of the conclusions.

2. Methods

In this study, we leverage a statistical approach to identify and rank the source areas of rapid flow-like landslides and a conceptual model to simulate their runout. The flowchart in Fig. 1 outlines the four stages of our proposed methodology, applied to the Italian railway network. The first stage involves data preparation, which includes gathering (i) a Digital Elevation Model (DEM), (ii) a map of the transportation infrastructure under investigation (e.g., a railway network), and (iii) one or more landslide inventory maps for training and validating the LS models. The second stage ("procedure", the core of the methodology, in Fig. 1) encompasses the classification of landslides into channelized and hillslope movements, the identification and modeling of landslide source areas, and the simulation of flow runout. The third stage concentrates on the classification (i.e., ranking) of landslide susceptibility (LS) and the generation of railway exposure (RE) maps. Finally, the fourth stage addresses the validation of the LS and RE maps. To assess the "predictive performance" (in a validation sense, as per (Reichenbach et al. - 2018) of a landslide susceptibility model, it is advisable to utilize independent inventories for validation, as suggested by Steger et al. (2017). In the absence of a secondary inventory, an alternative approach involves dividing the available inventory into two subsets for training and validation. In the following sections, we provide a detailed description of each stage, except for data preparation, which is primarily a technical step.

2.1. Distinction between hillslope and channelized rapid flow-like landslides

The proposed methodology delineates distinct modeling approaches for channelized and hillslope rapid flow-like landslides, with the combination of their results resulting in a unified "combined" map.

Hillslope rapid flow-like landslides predominantly occur during rainfall events, often initiated by rills and/or shallow landslides, and typically originate in unconsolidated sediments along hillsides (Hürlimann et al., 2015). These phenomena can be initially referred to as "gravel/sand/debris slides," according to Hungr et al. (2014), and may be termed "debris avalanches." In this study, hillslope rapid flow-like landslides encompass phenomena classified as "debris flow in unchanneled basins" and "debris avalanches" as defined by Crosta et al. (1990).

Channelized rapid flow-like landslides frequently develop within steep and confined channels. The transported materials may originate directly from channel sediments (Gregoretti and Fontana, 2008), or result from failures in upstream or channel-side hillslopes. Channelized movements generally exhibit longer runouts (Hunter and Fell, 2003; Scotto di Santolo and Evangelista, 2009) and come to rest at lower slopes (Guthrie et al., 2010) compared to hillslope landslides. Hungr et al. (2014) classified these types of failures as "Debris flows" or "Mud flows," while, in accordance with Crosta et al. (1990), they partially fall within the categories of "debris torrents" and "debris flows in channeled basins," which typically have larger average catchment areas than unchanneled debris flows. A graphical and schematic representation of channelized and hillslope debris flows can also be found in Chen et al. (2009).

The classification of landslides into channelized and hillslope phenomena is executed through the subdivision of the study area into slope units (SU) (Alvioli et al., 2016). A slope unit is a non-uniform terrain partition defined by drainage and divide lines, aiming to maximize geomorphological consistency within each unit while ensuring heterogeneity between neighboring units (Alvioli et al., 2020). Considering this slope unit subdivision, we assume that a rapid flow-like landslide entirely contained within a slope unit can be categorized as a hillslope movement, whereas a rapid flow-like landslide intersecting the boundaries of a slope unit (typically defined by a drainage line) can be considered a channelized movement.

To distinguish between hillslope and channelized landslides, slope units are intersected with landslide polygons, and the area of the resulting polygons from the intersection is compared to a selected threshold. In cases where a single landslide (L) intersects multiple slope units, it can be subdivided into several polygons (L_1, L_2, …). Typically, a landslide is divided into two polygons. The area (A) of each polygon is then compared to the total area of the landslide ($R_1 = A(L_1)/A(L)$, $R_2 = A(L_2)/A(L)$, …); If all values of the ratios (R_1, R_2, …) are less than a threshold value set at 0.95, the landslide is classified as channelized. Otherwise (if any of the R_i values >0.95), the landslide is categorized as a hillslope flow-like movement.

2.2. Modeling landslide source areas

The training inventory map is used to identify the source areas (SA) of the rapid flow-like landslides using a probabilistic approach. To achieve this goal, having the delineation of source areas in the training landslides is essential. In cases where this data is unavailable due to the training inventory not differentiating between trigger areas and propagation/deposit areas, we assume that the source areas are situated in the highest regions of the landslide polygons. To pinpoint these upper sections within each landslide polygon, we extract only those cells with elevations exceeding the 90th percentile of the elevation distribution within the same polygon (Marchesini et al., 2020).

To evaluate the relative probability of each DEM grid cell to be a

source area, we adopt a "Topographic Threshold" (*TT*) approach, whose basics were reviewed and described by (Torri and Poesen, 2014). The set of functions considered in the study are shown in Table 1. Two different sets of *TT* functions are derived for channelized and hillslope movements. For this aim, we implemented an automated procedure (coded as a shell/GRASS/R script) capable to execute the following steps: (i) identification of the higher portion (raster cells) of each landslide (i.e., assumed as source area representative for the flow initiation zone); (ii) exclusion of raster cells with flow accumulation area less than a given threshold; (iii) evaluation of slope and flow accumulation area of the selected cells; and (iv) fitting a power law quantile regression equation defined as follows (Cavalli et al., 2017; Heinimann, 1998; Horton et al., 2008; Rickenmann and Zimmermann, 1993):

$$tan(\beta) = cA^b \quad (1)$$

where β is the slope, A is the flow accumulation area and c and b are empirical coefficients. The second step (exclusion of some raster cells) is devoted to include in the analysis only areas with non-negligible surface runoff, because rapid flow-like landslides occur on partially or fully saturated debris (Hungr et al., 2014), a condition that may be favored by the convergence of surface runoff.

The coefficients in Eq. (1) are obtained applying a quantile regression approach and considering the following percentile(quantile) values: 5%(0.05), 10%(0.1), 25%(0.25), 75%(0.75), 90%(0.90), 95%(0.95). Each set of coefficients identifies a different function for the flow accumulation i.e., $\beta_{05}(A)$, $\beta_{10}(A)$, $\beta_{25}(A)$, $\beta_{75}(A)$, $\beta_{90}(A)$, $\beta_{95}(A)$. Quantile regression computed for the 5% quantile identifies the curve that splits the data into 5% (below the curve) and 95% (above the curve). 50% of the data are between the $\beta_{25}(A)$, $\beta_{75}(A)$ curves and 15% between the curves $\beta_{75}(A)$ and $\beta_{90}(A)$. In the methodology, we assume that a generic source area (SA) is characterized by slope and drainage area values similar to those derived from the training inventory and fit by quantile regressions. Denoting by β_A the slope of a generic cell with a flow accumulation area A, Table 1 shows how the $\beta_{xx}(A)$ fits are used to classify raster cells according to a relative probability to be a source area. This raw yet empirical assumption, allowed to identify source area objectively.

The maximum relative probability of a raster cell to be a source area (SA) is set at 50% and the minimum at 5% (Table 1). Cells with terrain slope and flow accumulation area below $\beta_{05}(A)$ or above $\beta_{95}(A)$ have 0% probability to be a SA.

2.3. Landslide runout modeling

To model the propagation of rapid flow-like landslides, the methodology exploits "r.randomwalk" (Mergili et al., 2015)). The software implements a Monte Carlo approach to simulate rapid flow-like landslides paths from known source areas locations. Lateral spreading of the flow is controlled by the local slope and rules that force the perpetuation of the flow direction. Parameters used by r.randomwalk to select the possible paths followed by trajectories are well described in the original work by (Mergili et al., 2015). The trajectories are certainly driven by the direction of maximum slope but some spread (deviation) from that trajectory is allowed to prevent the flow from concentrating into an unrealistic linear feature. In particular, the randomness of the paths is handled by two parameters f_β and f_d, the value of which defines with what probability, during pixel-to-pixel routing, a cell may be affected by trajectories coming from one of the adjacent but higher-located cells. In this work, the values of f_β and f_d were assumed to be 5 and 2, respectively (values that are in agreement with the results of (Mergili et al., 2015)), and it was also supposed that a single trajectory is able to pass obstacles no higher than 5 m.

The software is able to simulate a large number of paths and the main output of "r.randomwalk" is an impact frequency map, which portrays the count of paths (*t*) for each raster cell.

A modeled path ends when a predefined "break criterion" is met. In r.randomwalk, several break criteria can be used, including empirical relationships based on volume of material released or flow velocity. However, since information on material released and flow velocity is not easy to estimate, in this work we use the *h/l* ratio break criterion, i.e. height/distance traveled, also referred to as reach angle (Corominas, 1996; Prochaska et al., 2008)).

In the proposed methodology, we firstly define the distribution of reach angles $\left(\Omega = atan\left(\frac{h}{l}\right)\right)$ using only the paths originated from the higher portion (§2.2) of landslides in the training dataset. In detail, Ω values are estimated by measuring *h* and *l* where the paths intersect (i.e. exit) the landslide boundaries and their statistical distribution is modeled with a Gaussian or lognormal distribution function ($F(\Omega)$) fitting the empirical data.

To simulate runout throughout the entire study area, all raster cells classified as SAs (§2.2) are exploited as runout initiation paths, which end at reach angle values randomly sampled from the distribution function ($F(\Omega)$). r.randomwalk allows the user to choose the maximum number of paths that can be initialized by each raster cell, which in the proposed methodology is reduced by multiplying it by the value of the relative probability calculated by the *TT* model. This allows to run different flow runout simulations from the different source area locations in dependence of their relative probability of being a potential source area.

2.4. Susceptibility and exposure

In the proposed methodology, landslide susceptibility classification is based on a measure of similarity, in terms of path counts (*t*), between each raster cell and those included in the training landslide polygons. More in detail, to convert the impact frequency map (§2.3) into a susceptibility map (LS map) to the runout of rapid flow-like landslides, we first extract the impact frequency values (*t*) within landslide polygons of the training inventory (Santangelo et al., 2021).

These values are then used to construct an empirical cumulative distribution function (ECDF(t)), which is applied to the impact frequency map to generate the LS map, assigning values from 0 to 1 to the raster cells. A value near 1.0 signifies a high susceptibility to the runout of flow-like landslides, indicating that the number of modeled paths through that cell is similar to the maximum paths in the training inventories. Conversely, values near zero indicate low or zero modeled path values, indicating low susceptibility.

ECDF(t) functions are defined separately for hillslope and channelized phenomena, and they are also used to assess the exposure of transportation infrastructure (RE) to rapid flow-like landslides. Specifically, (i) the transportation infrastructure is split into segments of equal length, (ii) then each segment is associated with the total number of paths (*t*) computed by r.randomwalk for the underlying raster cells, and (iii) finally the *ECDF(t)* function is applied to each segment to estimate its exposure value starting from the corresponding total number of paths (*t*). High values calculated with the ECDF curve (close to 1) indicate locations along the linear infrastructure with high concentration of runout paths, then having a high exposure level to flow-like landslides. Conversely, values close to 0 (low number of paths) correspond to locations with low exposure levels.

To create the final 'combined' LS map for rapid flow-like landslides, the methodology merges the LS maps for channelized and hillslope phenomena by selecting the higher value for each pixel. Similarly, the 'combined' exposure of the railway network (RE) is determined by choosing the highest RE value for each railway segment among those obtained for channelized and hillslope movements.

2.5. Validation of the susceptibility and exposure maps

The methodology uses two diversified approaches to validate the

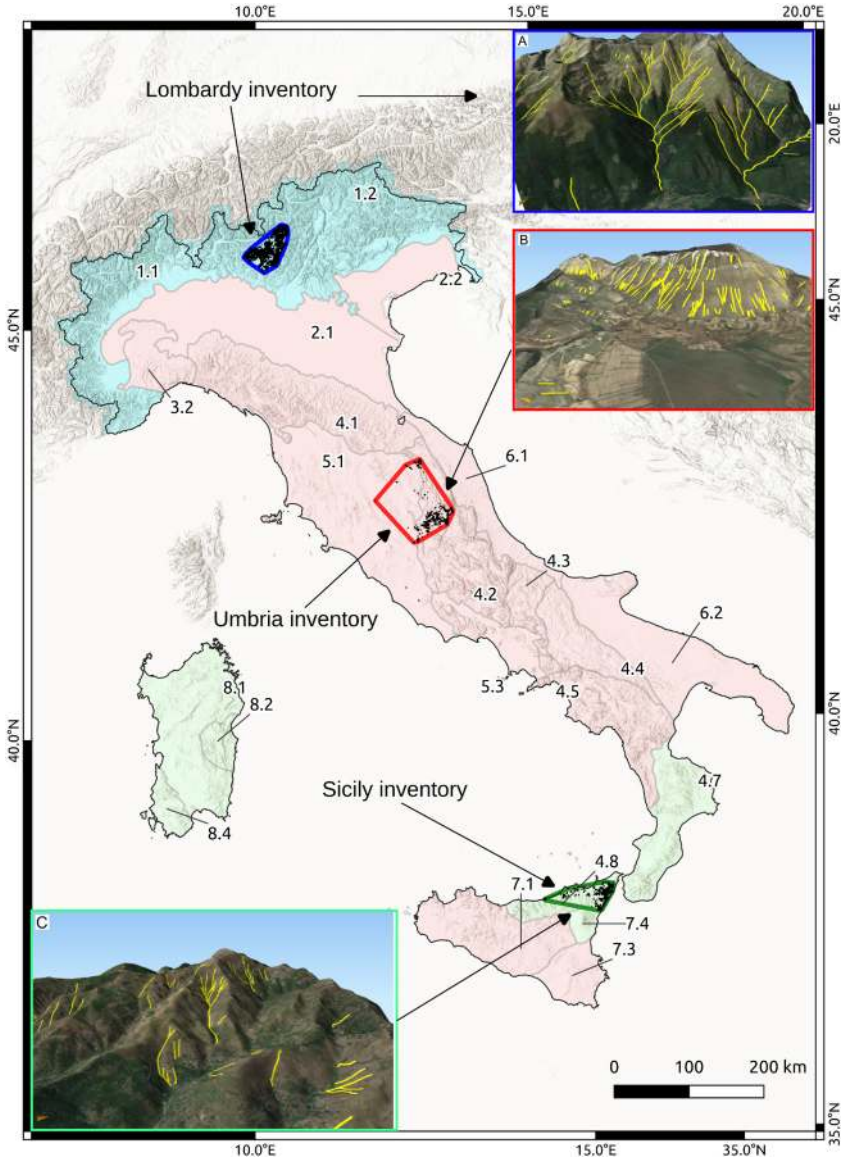

Fig. 2. Location of the training landslide inventory maps. In colors the convex hulls: blue = Lombardy inventories, red = Umbria inventory, green = Sicily inventory. The map shows the subdivision of Italy into topographic units (TU) as defined by (Guzzetti and Reichenbach, 1994). Light colors represent the heuristic associations of the topographic units with the training inventories: TU 1.1 and 1.2 is paired to Lombardy; TU 4.8, 7.4, 4.7, 8.1, 8.2, 8.4 to Sicily; and the remaining to Umbria (see §3.2.2). (For interpretation of the references to colour in this figure legend, the reader is referred to the web version of this article.)

landslide susceptibility map (LS map), and the transportation infrastructure exposure (RE) map, respectively. As suggested by (Reichenbach et al., 2018), multiple metrics are used to validate the modeling outputs. Validation uses an independent landslide dataset, not used for model training, which can be either a different landslide inventory or a landslide sample extracted from the original inventory.

LS map is validated using the Area Under the ROC curve (*AUROC*) and the Kolmogorov-Smirnov (*KS*) *'D'* statistic (Davis, 2002), which measures the maximum vertical distance between the empirical cumulative distribution functions (*ECDF*) of the susceptibility map in the independent landslide polygons and in the entire study area.

The ROC curve and AUC (Fawcett, 2006) are essential metrics in machine learning for evaluating and comparing classification models. The ROC curve illustrates how a binary classifier performs across various thresholds by plotting TPR (true positive rate) against FPR (false positive rate). The AUC condenses this performance into a single value ranging from 0 to 1, with 1 indicating a perfect classifier, 0.5 indicating random guessing, and values below 0.5 implying an inverse correlation with true labels. AUC is versatile, threshold-agnostic, and robust for assessing a model's ability to distinguish between positive and negative instances.

The second metric was introduced in this study, since it does not require information on no-landslide zones, which can prove useful in the cases where the landslide validation dataset has limited information.

The infrastructure exposure (RE) map is validated analyzing the spatial intersection between the transport infrastructure and the landslide validation polygons. In order to account for the width of the transportation infrastructure, the methodology requires the creation of a 3-m buffer around the equal-length linear segments into which the entire national rail network is divided. This is then overlaid on the landslide polygons to find the intersections.

If the distribution of RE values at landslide locations significantly differs from the overall network's RE distribution, it suggests that the RE zoning identifies some highly exposed railway segments. However, this validation approach relies heavily on the amount of data available in the validation dataset. Sufficient intersections between the railway network and validation landslides are necessary to establish a reliable frequency

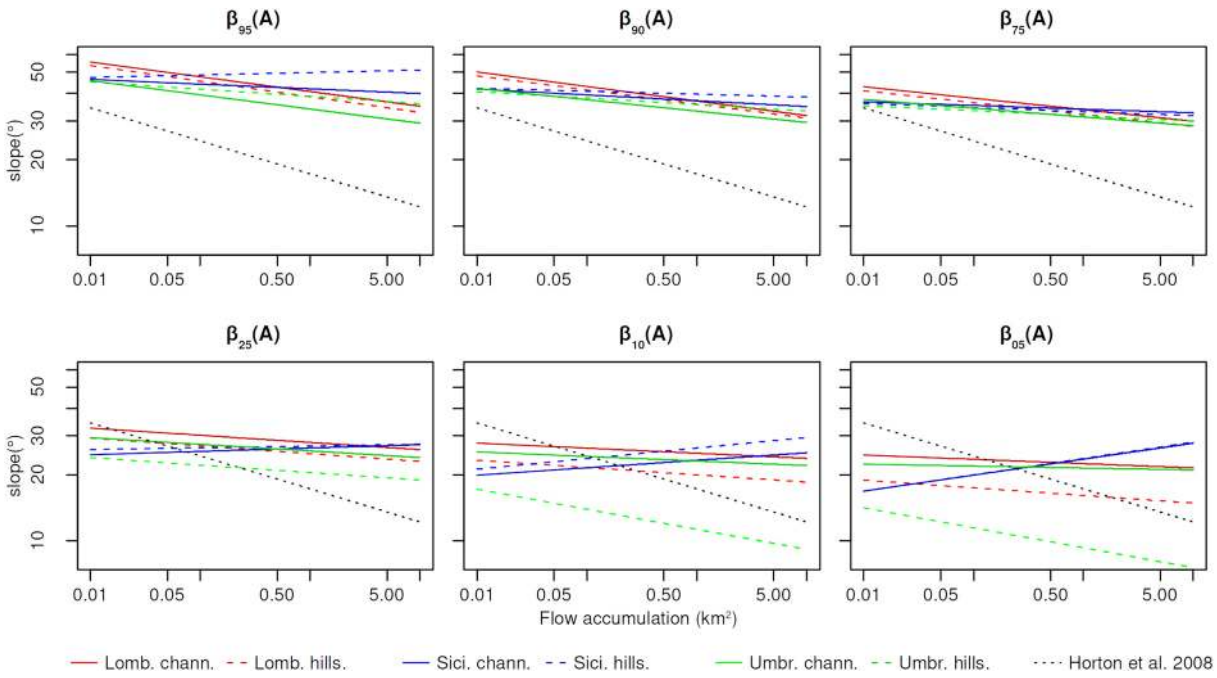

Fig. 3. Quantile regressions for different quantiles, inventories and rapid flow-like landslide types (from (Marchesini et al., 2020)). The dashed black line is the function proposed by Rickenmann and Zimmermann (1993) and used by (Horton et al., 2008).

distribution of exposure values for the intersected railway segments.

3. Case study: The Italian railway network

In Italy, the responsibility for maintaining the railway networks lies with the infrastructure manager, RFI (Rete Ferroviaria Italiana - https://www.rfi.it/en.html). RFI oversees the maintenance of approximately 17,700 km of railway tracks, a portion of which is susceptible to various natural hazards, including landslides (Alvioli et al., 2021; Firmi et al., 2021; Guzzetti et al., 2003; Salvati et al., 2018). The Italian railway network extends across the entire national territory, with recent findings (Firmi et al., 2021) indicating that roughly 7700 km of the network are potentially exposed to different types of landslides. The methodology detailed in the preceding section was applied comprehensively across the Italian territory to evaluate, at a national scale, the railway network's susceptibility to rapid flow-like landslides.

3.1. Data

In our case study, we employed the TINITALY Digital Elevation Model (DEM), recognized as the highest resolution DEM accessible at a national scale (Tarquini et al., 2007; Tarquini and Nannipieri, 2017), This DEM was created by combining, using the Mosaik process, of all available topographical data in Italy, sourced from maps at a scale of 1:25,000 or larger. The quality and spatial resolution of the DEM mirror the characteristics of the original data. Notably, in areas where triangulated points are widely spaced, the resulting triangle areas (Triangulated Irregular Network - TIN) are notably larger than the DEM resolution (10 m × 10 m) (Marchesini et al., 2021).

RFI (Rete Ferroviaria Italiana) provided the vector layer of the operational railway network, featuring a level of detail that allows for the representation of individual railway tracks, even within railway stations. Sections of the railroad located within tunnels were omitted from the dataset, as they are not susceptible to rapid landslides.

Training inventory of landslides data (Fig. 2) was obtained from three different geomorphological landslide inventories (Guzzetti et al., 2012; Marchesini et al., 2014), respectively, located in Lombardy, Umbria and Sicily regions (see Fig. 8 for the location and administrative region boundaries). The inventory in Lombardy was prepared at a scale of 1:10,000 for the Valcamonica and Valseriana basins, encompassing a total area of 2114 km^2 (blue polygon in Fig. 2). Landslides were recognized through visual interpretation of 1:33,000 black & white and 1:20,000 colour stereoscopic aerial photographs, and include 8110 segments representing landslide runouts.

The training inventory of rapid flow-like landslides in Umbria, which covers an area of about 8400 km^2, was prepared at 1:10,000 scale (red boundary in Fig. 2) through visual interpretation of 1:33,000 black & white and 1:13,000 colour stereoscopic aerial photographs, and includes a total of 1459 segments classified as rapid flow-like landslides. The training inventory in Sicily was prepared at 1:15,000 scale for an area of 1970 km^2 (green polygon in Fig. 2). The inventory was derived by interpreting b/w stereoscopic aerial photographs at 1:33,000 and 1:28,000 scale taken in 1954 and 2005, respectively (Bucci et al., 2016; Santangelo et al., 2015). The inventory includes a total of 1736 segments representing rapid flow-like landslides. In the three inventories the flow source areas are mapped as points and runouts as lines (Fig. 2). This type of mapping poses practical problems since the lines drawn by the photo-interpreters may not perfectly match the flow direction resulting from digital terrain models (DEMs) (Santangelo et al., 2015). To take into account graphical errors and facilitate modeling, a 20-m buffer was delineated around each segment.

For the validation, we use landslide polygons from the IFFI inventory map (Trigila et al., 2010), a national database published by the Istituto Superiore per la Protezione e la Ricerca Ambientale (ISPRA), available at the IdroGeo geoportal (https://idrogeo.isprambiente.it/app/). This inventory was already used to validate a national scale landslide non-susceptibility map (Marchesini et al., 2014) and a national map of landslide susceptibility (Loche et al., 2022). The IFFI inventory is a composite of different inventories prepared by the Italian regional administrations. The quality, density and accuracy of the inventory vary across the regions and also across the different landslide types as noted by (Loche et al., 2022). Only rapid flow-like landslides (i.e., those classified as "Rapid flows") were selected for the validation, corresponding to a total of 23,654 landslides (Fig. 5b).

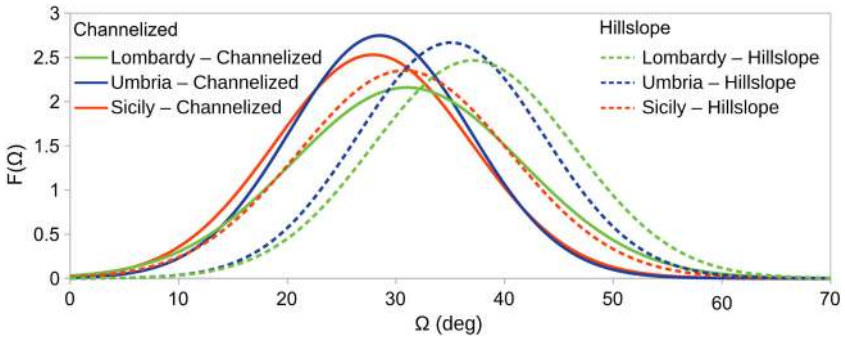

Fig. 4. Probability distribution functions ($F(\Omega)$) of the reach angle for the three inventories and the two types of rapid flow-like landslides.

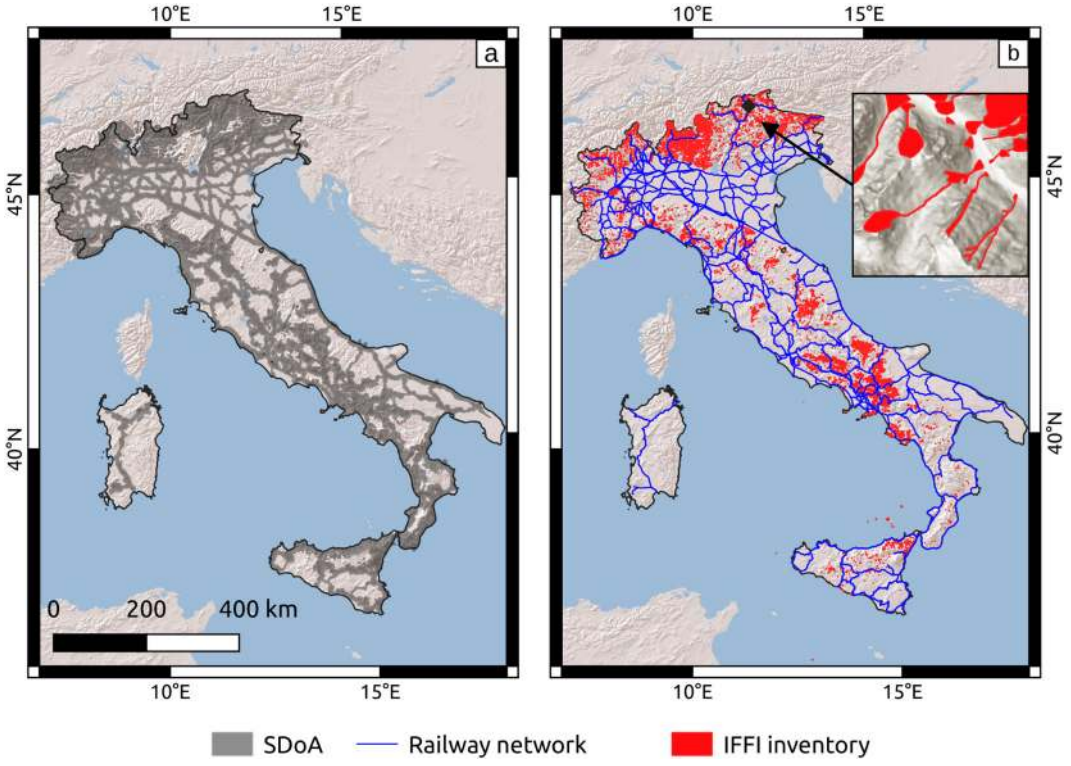

Fig. 5. a) Spatial domain of application (SDoA) of the methodology (see text for explanation). b) Railway network and IFFI inventory.

3.2. Modeling settings

3.2.1. Training settings

The classification of the training inventories for Lombardy, Umbria and Sicily into hillslope and channelized rapid flow-like landslides was based on the methodology described in §2.1, using the Italian slope units map produced by (Alvioli et al., 2020). The uppermost portion of each landslide polygon (10% of the cells at the highest elevation), was considered as landslide source area (SA, as explained in §2.2). To include only areas with non-negligible surface runoff, we excluded cells with flow accumulation area <500 m^2 (§2.2).

In Fig. 3 we show the results of six different quantile regressions (*TT* approach) obtained for channelized and hillslope movements, using the TINITALY DEM and the three training inventories (Lombardy, Umbria, and Sicily). The figure includes, for reference, the function proposed by (Rickenmann and Zimmermann, 1993) (and used by (Horton et al., 2008)), which is the lower limit boundary of the entire dataset collected by the authors.

To obtain $F(\Omega)$ (§2.3), we applied r.randomwalk with 100 paths from each cell of the landslide source areas identified in the training inventories, using the parameter values suggested by software authors (Mergili et al., 2015). We performed this step of the methodology for channelized and hillslope landslides (§2.4), independently, for the three training inventories (i.e. Umbria, Lombardy and Sicily). Fig. 4 shows the six modeled Gaussian probability distributions $F(\Omega)$ of the reach angle for the three inventories and the two landslide types.

3.2.2. Application settings

The runout modeling was not simulated over the whole country since the "railway density" is not homogeneous and is null in a few areas. To select the spatial domain of application (SDoA), we delineated the area draining towards the railway infrastructure (Fig. 5a). In addition, within the draining areas, we selected only raster cells with a ratio of elevation difference to planimetric distance from the railway, along the flow direction (Marchesini et al., 2021), equal to or higher than 2°. This value is precautionary, since debris flows rarely have reach angles $<4°$ (Rickenmann, 2005). We also excluded all raster cells with a hydrological distance from the railway network longer than a threshold of 10 km, which is a precautionary value compared to the maximum runout distance observed in the training inventories (i.e. 3500 m).

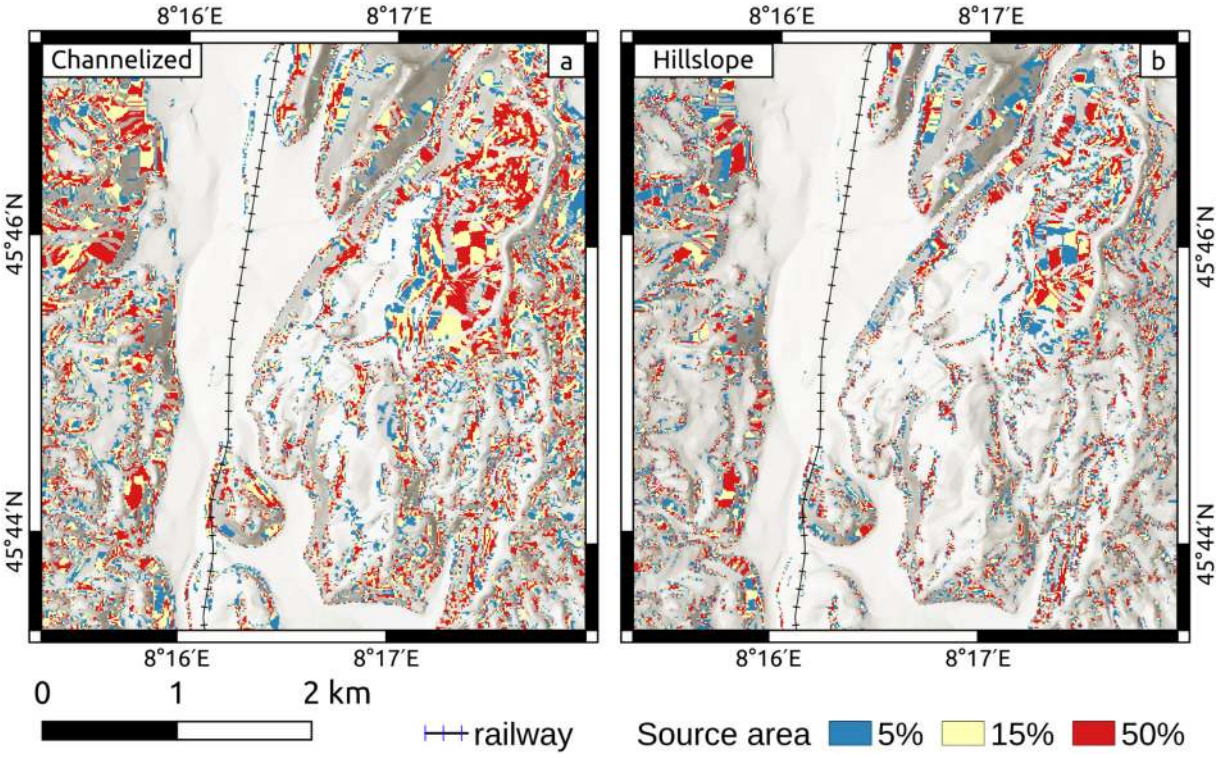

Fig. 6. Details of the maps of the relative probability to be source areas for (a) channelized and (b) hillslope rapid flow-like landslides.

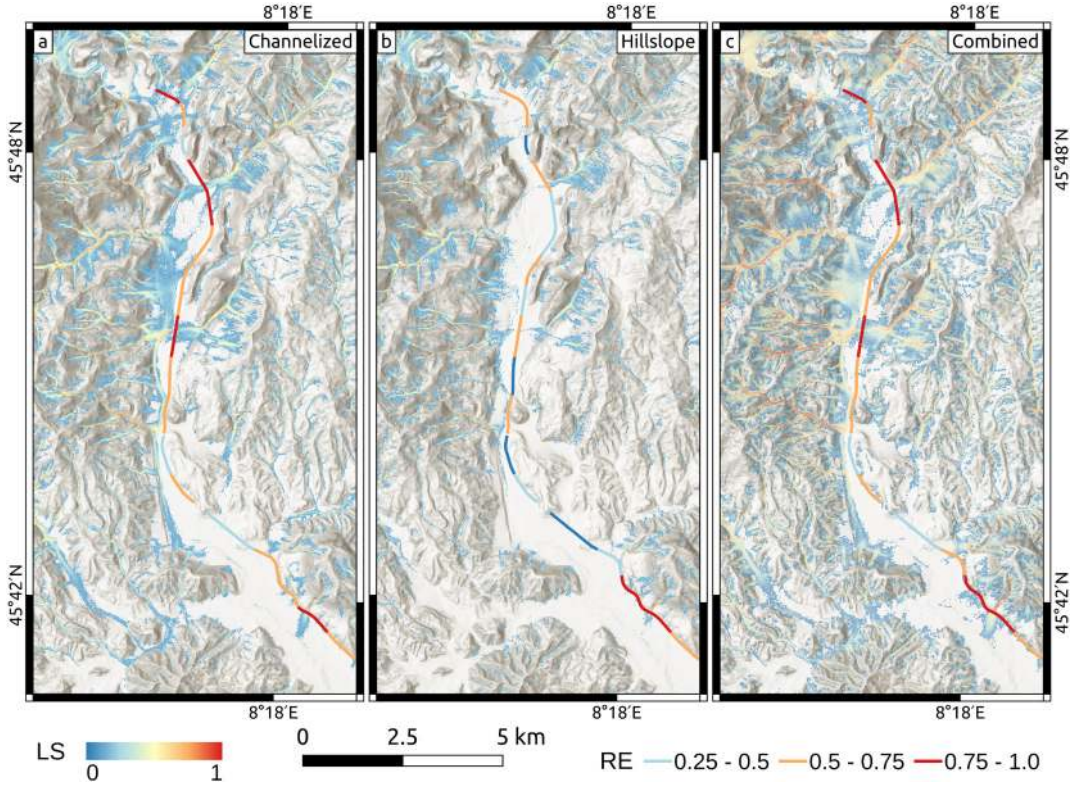

Fig. 7. Detail maps of the LS and RE maps. For LS, raster cells with values less or equal to 0.05 are not shown. (a) RE and LS for channelized flow-like landslides, (b) RE and LS for hillslope flow-like landslides, (c) LS and RE combined maps.

Since *TT* equations and $F(\Omega)$ models were calibrated in the three training areas (Lombardy, Umbria, and Sicily) shown in Fig. 2, their application to other parts of the country could be done only after pairing the training areas with different SDoA portions. Pairing was based on expert judgment considering geomorphological, climatic, and lithological characteristics. Among the different subdivisions of the Italian

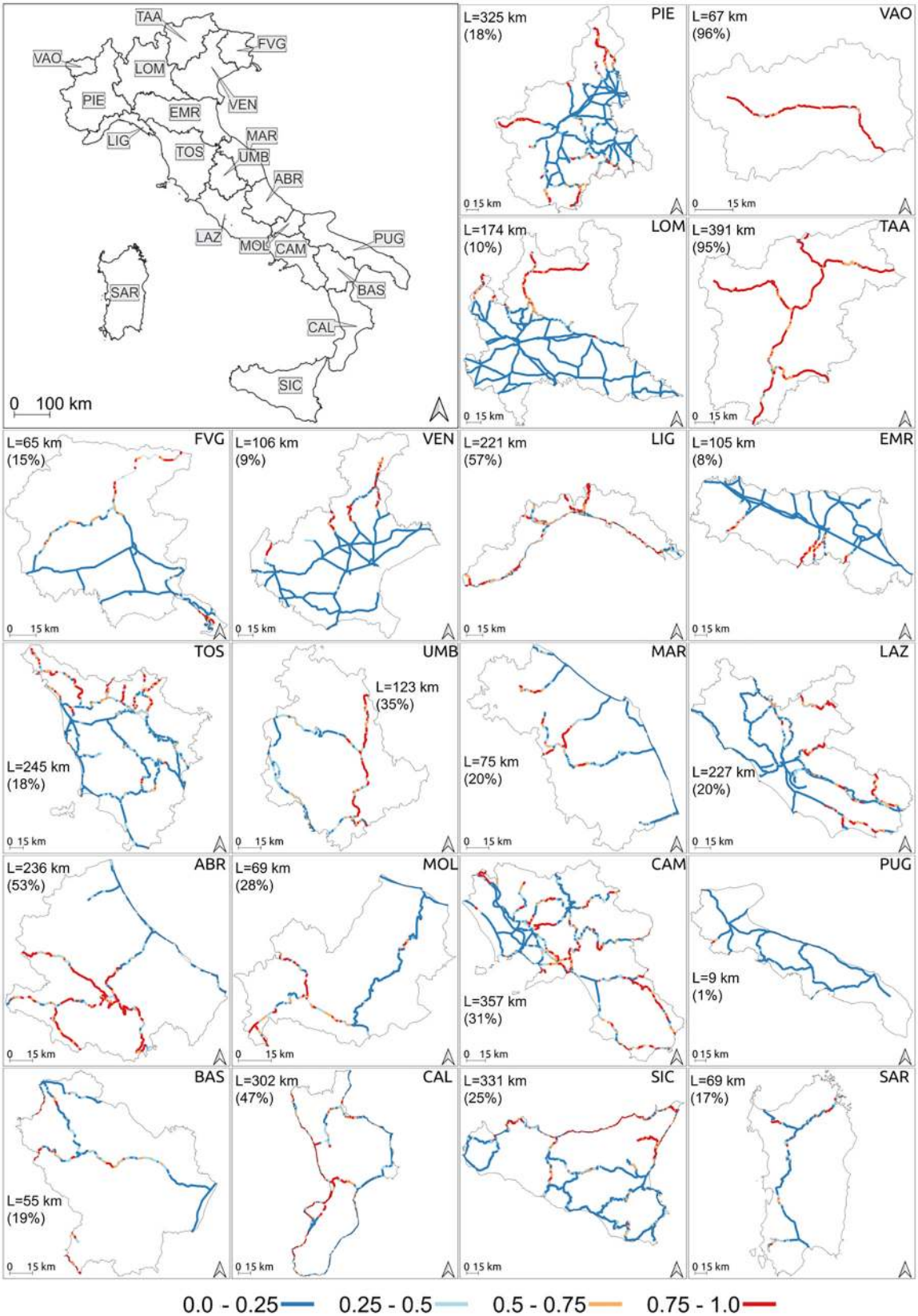

Fig. 8. Railway exposure (RE) to rapid flow-like landslides in the different Italian regions. The provided numerical values represent the linear extent of railway segments where the exposure exceeds 0.5, along with the corresponding proportion relative to the overall length of the railway line. Abruzzo (ABR); Calabria (CAL); Emilia-Romagna (EMR); Liguria (LIG); Veneto (VEN); Molise (MOL); Umbria (UMB); Marche (MAR); Lombardy (LOM); Campania (CAM); Friuli Venezia Giulia (FVG); Valle d'Aosta (VAO); Lazio (LAZ); Piedmont (PIE); Trentino-Alto Adige (TAA); Tuscany (TOS); Sicily (SIC); Basilicata (BAS); Apulia (PUG); Sardinia (SAR). Colors and ranges of RE values correspond to the following classes of exposure: *negligible, low, moderate, high, and very high*.

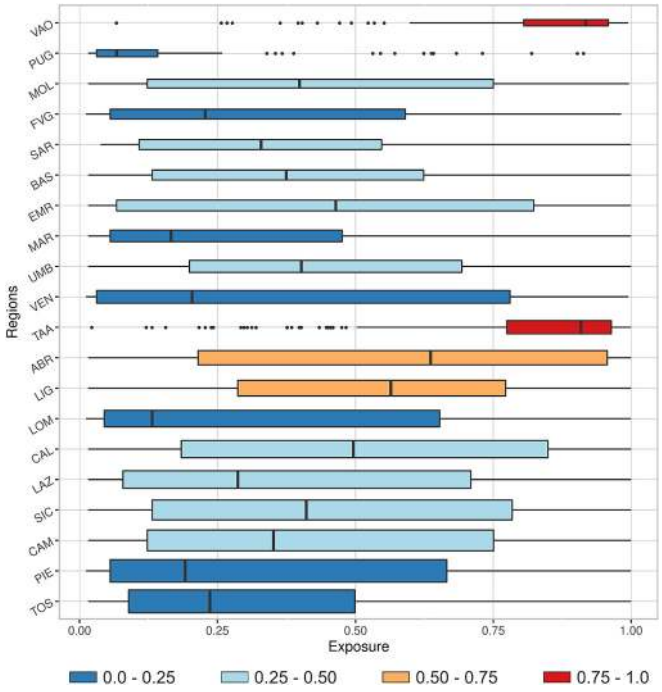

Fig. 9. Box plots showing the distribution of the railway exposure (RE) values of the segments in the regions of Italy (see Fig. 7). Width of boxplots is proportional to the fraction of rail segments in each region. Colors depend on the median value and are classified according to Fig. 7 (the *negligible* class is merged into *low*).

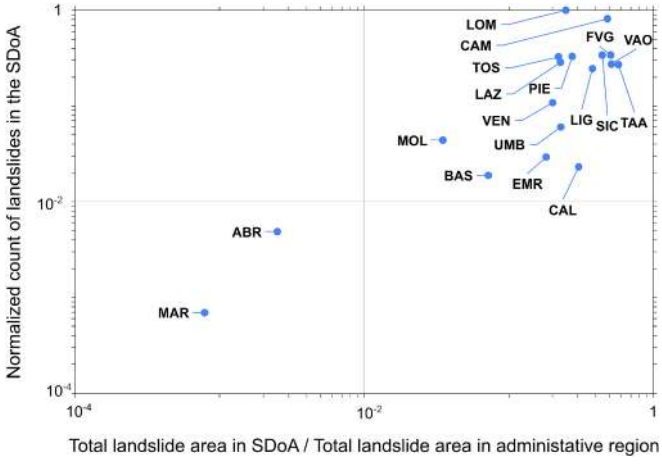

Fig. 10. The graph shows the landslides count and the relative area density in the SDoA across different regions. Marche and Abruzzo show significant differences with respect to the other regions.

territory (e.g. (Bini, 2013; Fredi and Lupia Palmieri, 2017)), we adopted the topographic and geomorphological physiographic units proposed by Guzzetti and Reichenbach (Guzzetti and Reichenbach, 1994). Fig. 2 portraits the final heuristic pairing between the three training inventories and the physiographic units and shows, as an example, that the entire Alpine chain (physiographic units 1.1 and 1.2) is associated with the Lombardy inventories.

The railway network was split into 1-km segments for RE assessment.

4. Results and discussion

Loche et al. (2022) found that the northern part of Italy, dominated by the Alpine arc, is highly susceptible to flow-like landslides due to steep terrain and elevation. However, mountainous terrain across the Italian peninsula creates conditions favorable for landslide occurrence. This emphasizes the need to evaluate the vulnerability of transportation infrastructure to such events nationwide.

Our methodology enables assessment of transportation network susceptibility to rapid flow-like landslides, demonstrated using the Italian railway network (Fig. 5). Proper modeling of source areas, runouts, and rigorous validation are crucial. Consequently, assessing prediction accuracy is essential to ensure reliable modeling of landslide zonation.

4.1. Rapid flow-like landslides source areas and runout

Landslides source areas and runout have been modeled according to the procedure described in §2.2 and §2.3, obtaining, respectively, topographic threshold (*TT*) functions and reach angles distributions ($F(\Omega)$).

Fig. 3 depicts the *TT* quantile regression functions for hillslope and channelized landslides, used to assess the likelihood of a raster cell being a source area for rapid flow-like landslides. It is observed that:

- For the Lombardy and Umbria training inventories, a negative correlation between flow accumulation and slope is evident across all quantile regression functions of the *TT* model, with a more pronounced effect in Lombardy.
- In Sicily, this correlation is primarily observed in equations corresponding to higher quantiles (95th, 90th, and 75th for channelized landslides; 90th and 75th for hillslope movements).
- In Lombardy, channelized landslides occur at steeper slope angles compared to hillslope landslides for all flow accumulation values. A similar trend is observed in Umbria for quantiles equal to or less than the 25th quantile.

The intermediate modeling results yields intriguing findings. Most quantile regressions derived from the *TT* approach confirm the established negative correlation between flow accumulation and slope for source areas (SAs) of rapid flow-like landslides (Chen et al., 2009; Horton et al., 2008; Rickenmann and Zimmermann, 1993). This result, however, was not necessarily expected, as the data used for regression fitting primarily stemmed from automatic cell selection in higher topographic regions of the training landslides.

Another noteworthy observation comes from equations $\beta_{05}(A)$ and $\beta_{95}(A)$ (Fig. 3), delineating flow accumulation and slope conditions expected within flow-like landslide source areas. While intuitively, SAs are rare on gentle slopes, interpreting their scarcity on steep slopes is less straightforward. We attribute this to the lack of vegetated and unvegetated soils/debris on very steep cliffs available for mobilization (Carrara et al., 2008).

The probability distributions $F(\Omega)$ of reach angles computed for the three inventories and two types of landslides (channelized and hillslope) exhibit similarities but not equality. Analysis (Fig. 4) reveals:

- Reach angle values, for channelized landslides, are generally lower than those for hillslope landslides.
- Sicily generally shows lower reach angle values than Umbria and Lombardy. In fact, the modes of the distributions of the reach angle values are always lower than in the other two regions and have significant values even below 10°.
- For channelized landslides, the central value of the distribution is around 30°, while it is 3–7° larger for hillslope landslides (Umbria: 35.1°, Sicily: 30.8°, Lombardy: 37.1°). Rickenmann (2005) reported the lowest travel angle for debris flows in fine material as 4° in a Swiss inventory, which is an unlikely value in our probability distributions. In fact, 4° corresponds to percentiles consistently smaller than 0.001 for channelized and smaller than 8×10^{-4} for hillslope landslides.

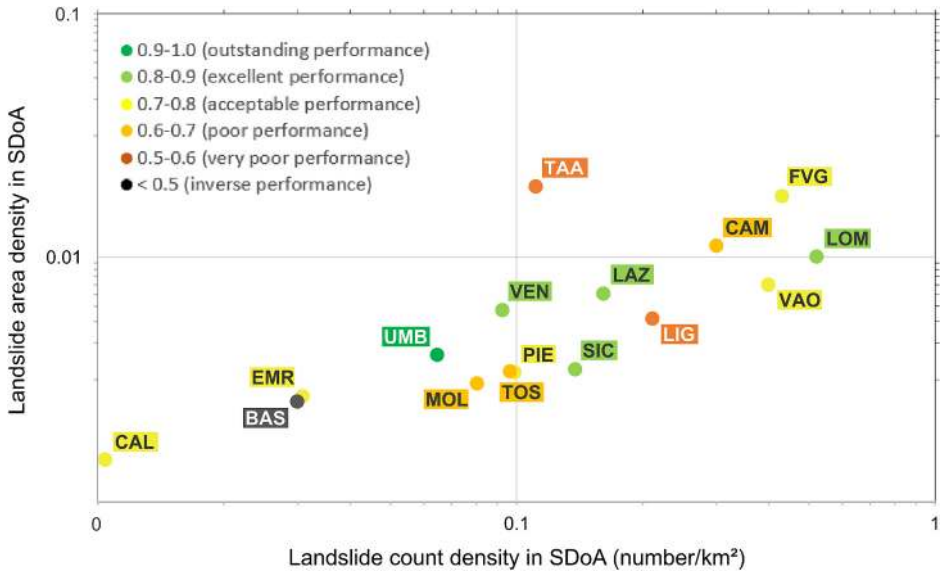

Fig. 11. Comparison of landslide count density and landslide area density in the SDoA. Colour (green, light green, yellow, orange, red and black) refers to 6 different ranges of Area Under the ROC (*AUROC*) values. (For interpretation of the references to colour in this figure legend, the reader is referred to the web version of this article.)

Interestingly, we found that automatically distinguishing between hillslope and channelized slope, based solely on intersection with a slope unit map, led to subtle differences in SA identification and runout propagation. In Lombardy, and to some extent in Umbria, the *TT* model indicated that, at the same slope, the flow accumulation required for channelized landslide initiation exceeds that for hillslope initiation (Fig. 3), consistent with experimental evidence (Crosta et al., 1990; VanDine, 1985).

Regarding flow propagation, Fig. 4 shows that channelized landslides generally have lower reach angle values compared to hillslope landslides, aligning with existing literature (Hunter and Fell, 2003; Lorente et al., 2003; Scotto di Santolo and Evangelista, 2009).

4.2. Rapid flow-like landslides susceptibility and railway exposure

Maps depicting landslide susceptibility and railway network exposure were produced following the methodology outlined in §2.4. Fig. 6 provides a small portion of the relative probability maps for rapid flow-like landslide source areas, highlighting distinct spatial patterns for channelized and hillslope occurrences.

The susceptibility maps (LS maps) for channelized and hillslope rapid flow-like landslides serve as intermediate results for the combined susceptibility map. Fig. 7 highlights differences between the two, notably longer propagation distances in channelized features. High susceptibility values (near 1) indicate areas with numerous runout paths and high susceptibility to flow-like propagation (e.g., the apical portion of a fan), while values near zero signify fewer paths and less susceptibility.

Fig. 8 depicts Italy's administrative subdivision into 20 regions alongside maps illustrating railway segment exposure in each region. RE is categorized into five levels: negligible (0.0–0.1), low (0.1–0.25), moderate (0.25–0.5), high (0.5–0.75), and very high (0.75–1.0). The letter "L" denotes the length of high to very high exposed railway lines, with value of RE $>$ 0.5, while percentage value refers to the corresponding percentage relative to the entire length of the railway network within this specific region. Regions with maximum exposed segments include TAA, CAM, SIC, PIE, and CAL, while regions such as PUG, BAS, FVG, VAO, SAR, and MAR have exposed segments totaling $<$100 km.

Fig. 9 displays boxplots illustrating the distribution of RE values across different Italian regions. In other words, Fig. 9 is complementary to Fig. 8, and sheds light on the details of the exposed segment situation in terms of value distribution on a 0–1 scale. The thickness of each boxplot corresponds to the total number of segments in the region, while colour indicates the median value. VAO and TAA, situated entirely in the Alpine chain, exhibit nearly all railway segments highly exposed to potential flow phenomena. ABR and LIG, also mountainous regions, show high average RE values. While most regions have low or moderate median RE values, some segments within them display high to very high exposure. PUG stands out as the only region characterized by consistently low RE values. It is worth noting that the longer the boxplot shape, the less representative its median value, especially if the distribution is clearly non-Gaussian, as in the case of LOM and VEN.

4.3. Validation of the susceptibility and exposure maps

To validate the landslide susceptibility (LS) and the railway exposure (RE) maps, we exploited the procedure described in §2.5, using the IFFI inventory as an independent validation dataset.

4.3.1. LS map validation

Due to the significant heterogeneity of the IFFI dataset, LS map validation was conducted region by region. To ensure accurate interpretation of results and mitigate potential misinterpretation stemming from varying landslide data abundance, an exploratory analysis of the IFFI data was initially conducted. This analysis aimed to compare regional IFFI inventories based on two variables: (i) the number of IFFI landslides within the SDoA and (ii) the percentage of SDoA area occupied by IFFI landslides relative to the entire region. Fig. 10 illustrates variable values, with the number of IFFI landslides within the SDoA normalized to the maximum value observed in Lombardy (1443 landslides) for improved graph clarity.

The IFFI dataset shows considerable variation in the abundance of rapid flow-like landslides across Italian regions, particularly evident between Marche and Abruzzo (MAR and ABR) and the rest of the country. Consequently, validation was performed for only 16 out of 20 Italian regions (as depicted in Fig. 8). MAR and ABR were excluded due to limited data availability, while PUG and SAR were omitted because of the absence of rapid flow-like landslides in the SDoA. BAS and CAL have the fewest landslides in the SDoA (27 and 33, respectively), while, at the opposite, LOM and CAM exhibit the largest amounts of landslide

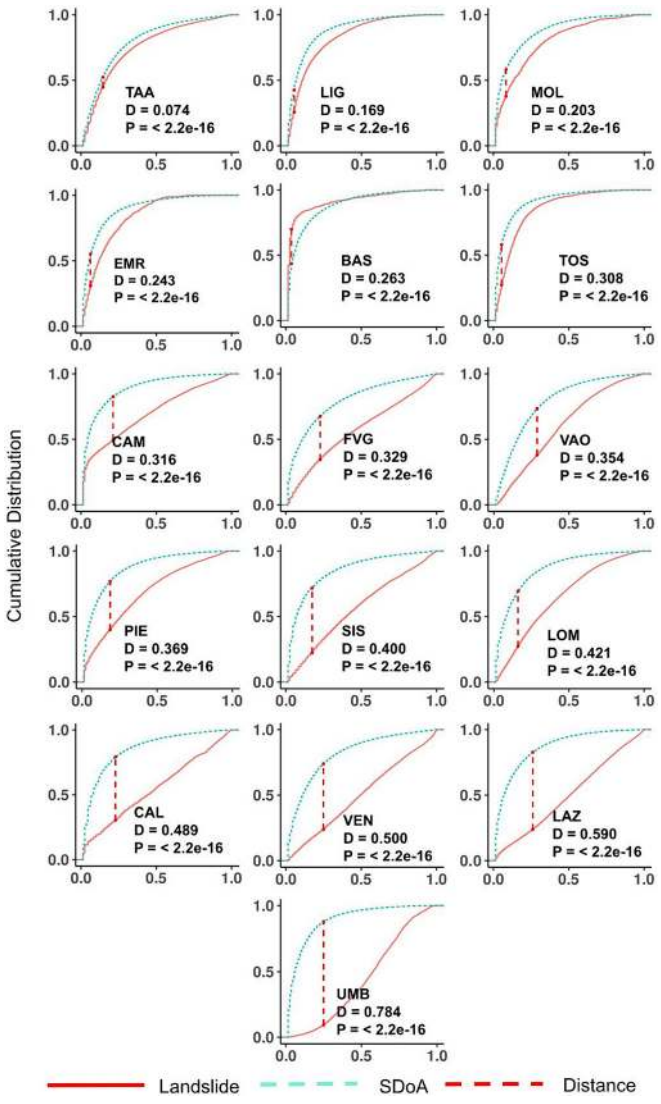

Fig. 12. *ECDF* of LS map values inside (i) the IFFI inventory (red curve) and (ii) the SDoA (blue curve), for the different administrative regions. Vertical dashed lines represent the *KS 'D'* statistic. The 'D' values and the related significance level of the *KS* test are also given. (For interpretation of the references to colour in this figure legend, the reader is referred to the web version of this article.)

movements within the SDoA (1443 and 1174, respectively).

Given these disparities in landslide information, we investigated whether a relationship existed between the density of landslide information within SDoAs and model predictive performance, measured by the AUROC index. In Fig. 11 colors depend on the *AUROC* values while *x* and *y* axes portray the IFFI landslide count density and the IFFI landslide area density in the SDoA, respectively. Although a positive correlation between the two axes is observed, TAA notably deviates from other regions. However, overall, there is no clear evidence of a direct relationship between landslide information density and LS map predictive performance.

Furthermore, the analysis of Fig. 11 provides insights into LS map validation results. Performance varies from acceptable to outstanding in 10 regions (UMB, LAZ, VEN, LOM, CAL, FVG, SIC, PIE, VAO, EMR), including the three regions with available landslide training inventories (LOM, UMB, SIC). Conversely, performance is poor in TOS, MOL, CAM, and very poor in LIG and TAA. BAS exhibits puzzling model performance with an AUROC value of 0.40. This indicates a lack of clear correlation between validation landslide density and model performance, highlighting that the reasons for the models' poor predictive performance may not be related to the abundance but to the quality of landslides information.

We decided to further assess the performances of the LS map. An additional test compares the empirical cumulative distribution (ECDF) of susceptibility values in the entire LS map with those in the landslide inventory polygons (§2.5). Fig. 12 displays the *ECDF* curves for each region alongside the KS 'D' metric. The *KS 'D'* statistic (Davis, 2002) measures the maximum vertical distance between the *ECDFs* of susceptibility values within independent landslide polygons and those across the entire study area. A notably large 'D' indicates significant dissimilarity between the two functions, suggesting differences in susceptibility values within the validation inventory polygons compared to the broader region, as expected for a susceptibility map. Conversely, a very small 'D' suggests random sampling of susceptibility values by landslide polygons, pointing at potential biases in either the susceptibility map, the landslide inventory, or both. The advantage of using the ECDF lies in its ability to autonomously evaluate model performance, even with limited validation data and without the need for binary representation of the dependent variable (value of 0 as non-landslide locations).

In Fig. 12, we note significant and varied disparities between the two distributions across regions. The anomalous AUROC value observed for BAS (Fig. 11) is corroborated by the inversion of the ECDFs: the distribution of LS map values within landslide polygons (red curve) surpasses that of the entire SDoA (blue curve). Furthermore, the maximum values of the KS 'D' statistic correspond to UMB (0.78) and LAZ (0.59), while the lowest correspond to TAA and LIG. We note that the two validation metrics for the LS map, AUROC and KS 'D' statistic, yield consistent results. KS 'D' confirms most AUROC findings, reinforcing good validation performance for UMB and LAZ and poor results for TAA, LIG, MOL, and TOS (Fig. 12).

In CAL and EMR, regions with similar low landslide density, intermediate AUROC values (0.7 to 0.8) indicate acceptable discrimination. Notably, CAL shows a high KS 'D' value (0.489), ranking fourth among all regions, while EMR has the fourth lowest KS 'D' value (0.243) (Fig. 12).

As an effort to elucidate the factors contributing to the LS map's low validation performance, as measured by at least one metric, we carried out an in-depth visual analysis of the classification and locations of IFFI landslides in specific regions (BAS, LIG, TAA, and additionally TOS, MOL, CAM). The same analysis has been carried out in an attempt to understand the reasons behind the high performance achieved in other regions (UMB, LAZ, but also SIC, LOM, VEN).

In the BAS region (Fig. 13a), numerous IFFI landslides on gentle slopes are classified as very or extremely rapid movements. A visual inspection reveals characteristics typical of earthflows, gravel/sand/debris slides, clay/silt slides, or complex landslides with limited runout. These features align with the region's terrain and geological composition, which primarily consists of hilly and low mountainous terrain composed of unconsolidated clastic rock, chaotic-melange, and siliciclastic sedimentary rocks (Bucci et al., 2022). Similar observations hold for the TOS, MOL, and partially in the CAM regions.

In the LIG region (Fig. 13b), large landslides occur on moderate slopes (~14°) and exhibit shapes inconsistent with rapid or very rapid landslides, resembling earthflows and complex slides instead.

In the TAA region (Fig. 13c,d), the IFFI polygons classified as rapid flow-like failures often encompass the entire upstream catchment of the landslide deposits, including many cells that the LS map does not classify as having high runout susceptibility and resulting in low validation performance.

Limited landslide data in regions like EMR (Fig. 13e,f), with only 42 landslides, pose challenges despite correct landslide type and morphology classification. The absence of analogous morphological settings in the training dataset (Umbria inventory, Fig. 2) contributes to poor model performance. In EMR, rapid movements mainly occur in badlands, prevalent in the Chaotic-mélange lithotype (Bucci et al., 2022)

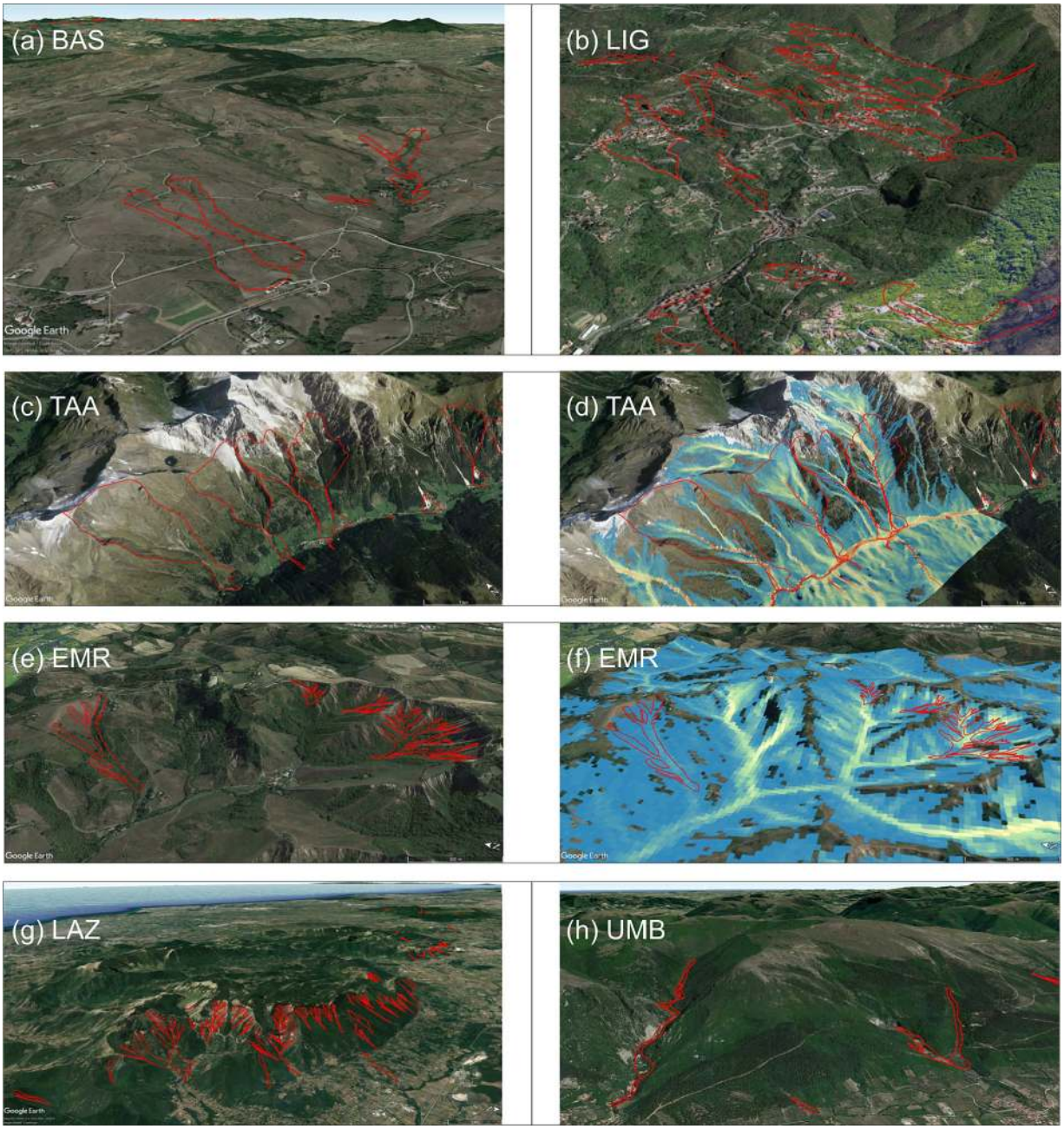

FIg. 13. Examples of landslide polygons classified as rapid and very rapid flows in the IFFI inventory. In BAS (a) and LIG (b) the polygons are poorly compatible with those typically generated by rapid flow-like landslides. In TAA (c)the source areas of the phenomena include the entire hydrological basin, causing many false positives where the LS map does not identify source areas and/or runout channels (d). In EMR (e,f) the LS map is not able to spatially predict the location of rapid flow-like landslides. In LAZ (g) and UMB (h) the landslide polygons are consistent with those expected for rapid flow-like landslides.

of EMR but not in UMB.

We conclude that issues in (i) mapping approaches, (ii) ambiguous landslide classification and (iii) inadequate representativeness of the training data, may explain the suboptimal predictive performance in certain regions (Figs. 11, 12).

In contrast, outstanding (as in UMB region) and excellent (as in LAZ, SIC, LOM, VEN regions) performances (Figs. 11, 12) are attributed to appropriate classification, location, and graphical representation of rapid flow-like landslides (Fig. 13g,h).

4.3.2. Railway Exposure map validation

To validate the RE map, we compared the distribution of exposure values for segments of the railway network intersecting with the IFFI inventory to that of all railway segments.

Regions with the highest number of intersections are: LOM (16), TAA (10), CAM (10), and VAO (7). Others have fewer intersections: SIC, PIE, and FVG (3 each), VEN and LAZ (2 each), and TOS, LIG, and BAS (1 each).

Fig. 14 depicts the relative frequency of exposure values for (i) all rail network segments and (ii) only those intersecting IFFI landslides. Excluded from the chart are railway segments in alluvial plains, where rapid flow-like landslides are not expected. The distributions of the two groups of segments differ significantly: those intersecting landslides tend to have exposure values mostly above 0.5, with a main mode near 1.0, while the entire railway network distribution peaks near 0 with denser information below 0.5. This stark contrast confirms the RE map's

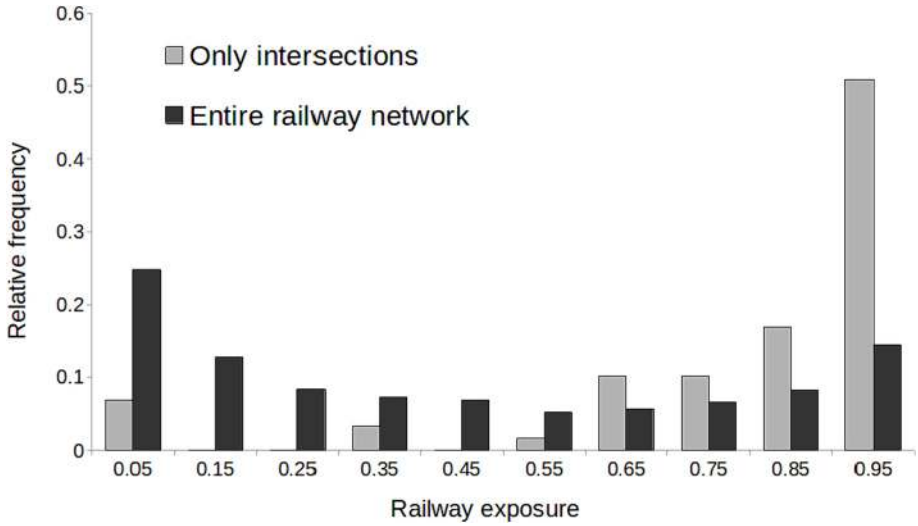

Fig. 14. Relative frequency of the railway segments included in different intervals of the exposure value for (i) segments overlaid by IFFI rapid flow-like landslides and (ii) all the segments of the railway network (excluding those located in alluvial plains).

strong prediction capability.

4.4. Limitations of the proposed procedure

The method presented in this research is versatile yet data-dependent, relying on digital terrain models and robust landslide inventories for large-scale assessments. While RE and LS maps primarily serve as ranking tools for exposure and susceptibility, aiding in prioritizing further studies and actions, limitations arise when local factors or transient conditions affect susceptibility.

The methodology objectively classifies training inventories into hillslope and channelized rapid flow-like landslides using slope units, treating both inventories separately due to distinct triggering and runout characteristics. However, caution is needed when merging susceptibility and railway exposure to avoid too many false positives.

Potential false negatives in RE and LS maps, may stem from various factors, including DEM inadequacies, *TT* model limitations in recognizing source areas, and non-representative training landslide inventories affecting source area characterization and reach angle calibration.

A methodology's advantage lies in classifying source areas solely based on information from landslide triggering zones, eliminating the need to identify non-source areas. However, subjectivity may arise in assigning relative probabilities to source areas. Additionally, slope and flow accumulation in source areas may not consistently correlate across all quantile regression functions.

Applying the method to the Italian railway network reveals certain limitations. Landslides in the training inventory are represented as lines, with buffer zones around each line used for training reach angle values. Small buffer sizes in some cases led to early path intersections with the buffered training polygons, resulting in high or very high reach angles.

Segmenting the railway into 1 km sections for exposure assessment through random path intersections introduces subjectivity, potentially impacting exposure evaluation. We adopted 1 km segments in line with Alvioli et al. (2021) to balance critical section identification while highlighting the significance of even low exposure values in short railway segments. This is particularly relevant in areas where the railway crosses debris flow fans, where individual short segments (even 10–20 m) may seem to have low exposure due to a relatively low chance of direct rapid flow-landslide intersection. However, for the broader railway section within the debris flow fan, exposure remains high, and any impact on a small segment within the fan can disrupt train operations along the entire longer section.

5. Conclusion

In conclusion, our methodology for assessing transportation network exposure to rapid flow-like landslides has been successfully applied to the entire Italian railway network. Leveraging statistical and conceptual approaches, the model requires input data such as a transportation infrastructure map, a medium/high-resolution digital elevation model, and landslide inventories for training and validation purposes.

Key outputs include maps delineating landslide source areas, susceptibility to landslide runout, and exposure of transportation infrastructure. The model's effectiveness was demonstrated through validation against an extensive landslide inventory covering the entire national territory.

Results indicate that approximately 20.1% of the Italian railway network exhibits exposure values exceeding 0.5 on a scale from 0.0 to 1.0, with around 13.4% classified as highly exposed (exposure >0.75) to rapid flow-like phenomena. These findings emphasize the significant challenges posed to infrastructure functionality and transportation safety.

Noteworthy insights from this research include the efficacy of high-quality landslide inventories for training models across expansive regions. Furthermore, the classification of hillslope and channelized rapid flow-like landslides is optimized by analyzing the intersection of landslide polygons with a suitable mapping of slope units. It is essential to recognize the distinctions in source areas and travel characteristics for hillslope and channelized landslides, warranting separate treatment and simulation.

In summary, this study underscores the importance of robust data inputs and nuanced modeling approaches for accurately assessing the exposure of transportation networks to rapid flow-like landslides, providing valuable insights for infrastructure management and safety planning.

Declaration of Generative AI and AIassisted technologies in the writing process statement

During the preparation of this work the authors used the Generative AI tool 'ChatGPT v.3.5,' developed by OpenAI, in order to improve readability and language. After using this tool, the authors reviewed and edited the content as needed and took full responsibility for the content of the publication.

CRediT authorship contribution statement

Ivan Marchesini: Writing – review & editing, Writing – original draft, Visualization, Supervision, Software, Project administration, Methodology, Investigation, Formal analysis, Data curation, Conceptualization. **Omar Althuwaynee:** Writing – review & editing, Writing – original draft, Visualization, Validation, Software, Investigation, Formal analysis. **Michele Santangelo:** Writing – review & editing, Resources, Data curation, Conceptualization. **Massimiliano Alvioli:** Writing – review & editing, Conceptualization. **Mauro Cardinali:** Writing – review & editing, Resources. **Martin Mergili:** Writing – review & editing, Software. **Paola Reichenbach:** Writing – original draft. **Silvia Peruccacci:** Writing – review & editing, Project administration, Funding acquisition. **Vinicio Balducci:** Software. **Ivan Agostino:** Resources, Funding acquisition. **Rosaria Esposito:** Resources, Funding acquisition. **Mauro Rossi:** Writing – review & editing, Software, Funding acquisition, Conceptualization.

Declaration of competing interest

The authors declare the following financial interests/personal relationships which may be considered as potential competing interests:

Ivan Marchesini reports financial support was provided by RFI (Gruppo Ferrovie dello Stato Italiane).

Data availability

1. DEM: TINITALY DEM is available here: http://tinitaly.pi.ingv.it/
2. IFFI inventory is available here: https://idrogeo.isprambiente.it/app/iffi?

Acknowledgements

This work was partially supported by RFI (Gruppo Ferrovie dello Stato Italiane), contract number 488, 01/02/2018.

The authors thank Dr. Fausto Guzzetti for his advice and insightful comments.

The responsibility for the content and any remaining errors remains exclusively with the authors.

Appendix A. Supplementary data

Supplementary data to this article can be found online at https://doi.org/10.1016/j.enggeo.2024.107474.

References

Alvioli, M., Marchesini, I., Reichenbach, P., Rossi, M., Ardizzone, F., Fiorucci, F., Guzzetti, F., 2016. Automatic delineation of geomorphological slope units with <tt>r.slopeunits v1.0</tt> and their optimization for landslide susceptibility modeling. Geosci. Model Dev. 9 (11), 3975–3991. https://doi.org/10.5194/gmd-9-3975-2016.

Alvioli, M., Guzzetti, F., Marchesini, I., 2020. Parameter-free delineation of slope units and terrain subdivision of Italy. Geomorphology 358, 107124. https://doi.org/10.1016/j.geomorph.2020.107124.

Alvioli, M., Santangelo, M., Fiorucci, F., Cardinali, M., Marchesini, I., Reichenbach, P., Rossi, M., Guzzetti, F., Peruccacci, S., 2021. Rockfall susceptibility and network-ranked susceptibility along the Italian railway. Eng. Geol. 293, 106301 https://doi.org/10.1016/j.enggeo.2021.106301.

Alvioli, M., Falcone, G., Mendicelli, A., Mori, F., Fiorucci, F., Ardizzone, F., Moscatelli, M., 2023. Seismically induced rockfall hazard from a physically based model and ground motion scenarios in Italy. Geomorphology 429, 108652. https://doi.org/10.1016/j.geomorph.2023.108652.

Bini, C., 2013. Geology and geomorphology. In: Costantini, E.A.C., Dazzi, C. (Eds.), The Soils of Italy. Springer, Netherlands, pp. 39–56. https://doi.org/10.1007/978-94-007-5642-7_3.

Bornaetxea, T., Marchesini, I., Kumar, S., Karmakar, R., Mondini, A., 2022. Terrain visibility impact on the preparation of landslide inventories: a practical example in Darjeeling district (India). Nat. Hazards Earth Syst. Sci. 22 (9), 2929–2941. https://doi.org/10.5194/nhess-22-2929-2022.

Bozzolan, E., Holcombe, E.A., Pianosi, F., Marchesini, I., Alvioli, M., Wagener, T., 2023. A mechanistic approach to include climate change and unplanned urban sprawl in landslide susceptibility maps. Sci. Total Environ. 858, 159412 https://doi.org/10.1016/j.scitotenv.2022.159412.

Bucci, F., Santangelo, M., Cardinali, M., Fiorucci, F., Guzzetti, F., 2016. Landslide distribution and size in response to Quaternary fault activity: the Peloritani Range, NE Sicily, Italy. Earth Surf. Process. Landf. 41 (5), 711–720. https://doi.org/10.1002/esp.3898.

Bucci, F., Santangelo, M., Fongo, L., Alvioli, M., Cardinali, M., Melelli, L., Marchesini, I., 2022. A new digital lithological map of Italy at the 1:100 000 scale for geomechanical modelling. Earth Syst. Sci. Data 14 (9), 4129–4151. https://doi.org/10.5194/essd-14-4129-2022.

Cabral, V., Reis, F., Veloso, V., Ogura, A., Zarfl, C., 2023. A multi-step hazard assessment for debris-flow prone areas influenced by hydroclimatic events. Eng. Geol. 313, 106961 https://doi.org/10.1016/j.enggeo.2022.106961.

Carrara, A., Crosta, G., Frattini, P., 2008. Comparing models of debris-flow susceptibility in the alpine environment. Geomorphology 94 (3), 353–378. https://doi.org/10.1016/j.geomorph.2006.10.033.

Cavalli, M., Crema, S., Trevisani, S., Marchi, L., 2017. GIS tools for preliminary debris-flow assessment at regional scale. J. Mt. Sci. 14 (12), 2498–2510. https://doi.org/10.1007/s11629-017-4573-y.

Chen, J.-C., Lin, C.-W., Wang, L.-C., 2009. Geomorphic characteristics of hillslope and channelized debris flows: a case study in the Shitou area of Central Taiwan. J. Mt. Sci. 6 (3), 266–273. https://doi.org/10.1007/s11629-009-0250-0.

Corominas, J., 1996. The angle of reach as a mobility index for small and large landslides. Can. Geotech. J. 33 (2), 260–271. https://doi.org/10.1139/t96-005.

Corominas, J., van Westen, C., Frattini, P., Cascini, L., Malet, J.-P., Fotopoulou, S., Catani, F., Van Den Eeckhaut, M., Mavrouli, O., Agliardi, F., Pitilakis, K., Winter, M. G., Pastor, M., Ferlisi, S., Tofani, V., Hervás, J., Smith, J.T., 2014. Recommendations for the quantitative analysis of landslide risk. Bull. Eng. Geol. Environ. 73 (2), 209–263. https://doi.org/10.1007/s10064-013-0538-8.

Crosta, G., Guzzetti, F., Marchetti, M., Reichenbach, P., 1990. Morphological classification of debris-flow processes in South-Central Alps (Italy). Proc. VI Int. Congress IAEG 1565–1572.

Davis, J.C., 2002. Statistics and Data Analysis in Geology, 3rd ed. John Wiley and Sons, Inc.

de Lima Neves Seefelder, C., Koide, S., Mergili, M., 2017. Does parameterization influence the performance of slope stability model results? A case study in Rio de Janeiro, Brazil. Landslides 14 (4), 1389–1401. https://doi.org/10.1007/s10346-016-0783-6.

Fawcett, T., 2006. An introduction to ROC analysis. Pattern Recogn. Lett. 27 (8), 861–874. https://doi.org/10.1016/j.patrec.2005.10.010.

Felsberg, A., Poesen, J., Bechtold, M., Vanmaercke, M., De Lannoy, G.J.M., 2022. Estimating global landslide susceptibility and its uncertainty through ensemble modeling. Nat. Hazards Earth Syst. Sci. 22 (9), 3063–3082. https://doi.org/10.5194/nhess-22-3063-2022.

Firmi, P., Iacobini, F., Rinaldi, A., Vecchi, A., Agostino, I., Mauro, A., 2021. Methods for managing hydrogeological and seismic hazards on the Italian railway infrastructure. Struct. Infrastruct. Eng. 17 (12), 1651–1666. https://doi.org/10.1080/15732479.2020.1822883.

Fredi, P., Lupia Palmieri, E., 2017. Morphological Regions of Italy. In: Soldati, M., Marchetti, M. (Eds.), Landscapes and Landforms of Italy. Springer International Publishing, pp. 39–74. https://doi.org/10.1007/978-3-319-26194-2_5.

Freeborough, K.A., Diaz Doce, D., Lethbridge, R., Jessamy, G., Dashwood, C., Pennington, C., Reeves, H.J., 2016. Landslide Hazard Assessment for National Rail Network. Proc. Eng. 143, 689–696. https://doi.org/10.1016/j.proeng.2016.06.104.

Freeborough, K., Dashwood, C., Diaz Doce, D., Jessamy, G., Brooks, S., Reeves, H., Abbott, S., 2018. A national assessment of landslide hazard from outside Party Slopes to the rail network of Great Britain. Q. J. Eng. Geol. Hydrogeol. 52 (3), 312–319. https://doi.org/10.1144/qjegh2018-029.

Gariano, S.L., Guzzetti, F., 2016. Landslides in a changing climate. Earth Sci. Rev. 162, 227–252. https://doi.org/10.1016/j.earscirev.2016.08.011.

Gregoretti, C., Fontana, G.D., 2008. The triggering of debris flow due to channel-bed failure in some alpine headwater basins of the Dolomites: analyses of critical runoff. Hydrol. Process. 22 (13), 2248–2263. https://doi.org/10.1002/hyp.6821.

Guthrie, R.H., Hockin, A., Colquhoun, L., Nagy, T., Evans, S.G., Ayles, C., 2010. An examination of controls on debris flow mobility: evidence from coastal British Columbia. Geomorphology 114 (4), 601–613. https://doi.org/10.1016/j.geomorph.2009.09.021.

Guzzetti, F., Reichenbach, P., 1994. Towards a definition of topographic divisions for Italy. Geomorphology 11 (1), 57–74. https://doi.org/10.1016/0169-555X(94)90042-6.

Guzzetti, F., Reichenbach, P., Cardinali, M., Ardizzone, F., Galli, M., 2003. The impact of landslides in the Umbria region, Central Italy. Nat. Hazards Earth Syst. Sci. 3 (5), 469–486. https://doi.org/10.5194/nhess-3-469-2003.

Guzzetti, F., Mondini, A.C., Cardinali, M., Fiorucci, F., Santangelo, M., Chang, K.-T., 2012. Landslide inventory maps: new tools for an old problem. Earth Sci. Rev. 112 (1), 42–66. https://doi.org/10.1016/j.earscirev.2012.02.001.

He, J., Zhang, L., Xiao, T., Wang, H., Luo, H., 2023. Prompt quantitative risk assessment for rain-induced landslides. J. Geotech. Geoenviron. Eng. 149 (5) https://doi.org/10.1061/JGGEFK.GTENG-10980, 04023023.

Heinimann, H.R., 1998. Methoden zur Analyse und Bewertung von Naturgefahren. https://www.bafu.admin.ch/bafu/de/home/themen/thema-naturgefahren/naturgefahren–publikationen/publikationen-naturgefahren/methoden-zur-analyse-und-bewertung-von-naturgefahren.html.

Horton, P., Jaboyedoff, M., Bardou, E., 2008. Debris flow susceptibiliy mapping at a regional scale. In: Proceedings of the "4e Conférence Canadienne Sur Les Géorisques", pp. 1–8.

Horton, P., Jaboyedoff, M., Rudaz, B., Zimmermann, M., 2013. Flow-R, a model for susceptibility mapping of debris flows and other gravitational hazards at a regional scale. Nat. Hazards Earth Syst. Sci. 13 (4), 869–885. https://doi.org/10.5194/nhess-13-869-2013.

Hungr, O., Leroueil, S., Picarelli, L., 2014. The Varnes classification of landslide types, an update. Landslides 11 (2), 167–194. https://doi.org/10.1007/s10346-013-0436-y.

Hunter, G., Fell, R., 2003. Travel distance angle for "rapid" landslides in constructed and natural soil slopes. Can. Geotech. J. 40 (6), 1123–1141. https://doi.org/10.1139/t03-061.

Hürlimann, M., McArdell, B.W., Rickli, C., 2015. Field and laboratory analysis of the runout characteristics of hillslope debris flows in Switzerland. Geomorphology 232, 20–32. https://doi.org/10.1016/j.geomorph.2014.11.030.

Jaiswal, P., van Westen, C.J., Jetten, V., 2010. Quantitative assessment of direct and indirect landslide risk along transportation lines in southern India. Nat. Hazards Earth Syst. Sci. 10 (6), 1253–1267. https://doi.org/10.5194/nhess-10-1253-2010.

Jia, G., Alvioli, M., Gariano, S.L., Marchesini, I., Guzzetti, F., Tang, Q., 2021. A global landslide non-susceptibility map. Geomorphology 389, 107804. https://doi.org/10.1016/j.geomorph.2021.107804.

Laimer, H.J., 2017. Anthropogenically induced landslides – a challenge for railway infrastructure in mountainous regions. Eng. Geol. 222, 92–101. https://doi.org/10.1016/j.enggeo.2017.03.015.

Lan, H., Martin, C.D., Zhou, C.H., 2008. Estimating the size and travel distance of Klapperhorn Mountain debris flows for risk analysis along railway, Canada. Int. J. Sedim. Res. 23 (3), 275–282. https://doi.org/10.1016/S1001-6279(08)60025-6.

Liang, X., Ge, Y., Zeng, L., Lyu, L., Sun, Q., Sun, Y., Wang, X., 2023. Debris flow susceptibility based on the connectivity of potential material sources in the Dadu River Basin. Eng. Geol. 312, 106947 https://doi.org/10.1016/j.enggeo.2022.106947.

Lin, L., Lin, Q., Wang, Y., 2017. Landslide susceptibility mapping on a global scale using the method of logistic regression. Nat. Hazards Earth Syst. Sci. 17 (8), 1411–1424. https://doi.org/10.5194/nhess-17-1411-2017.

Lin, Q., Lima, P., Steger, S., Glade, T., Jiang, T., Zhang, J., Liu, T., Wang, Y., 2021. National-scale data-driven rainfall induced landslide susceptibility mapping for China by accounting for incomplete landslide data. Geosci. Front. 12 (6), 101248 https://doi.org/10.1016/j.gsf.2021.101248.

Liu, K., Wang, M., Cao, Y., Zhu, W., Yang, G., 2018. Susceptibility of existing and planned Chinese railway system subjected to rainfall-induced multi-hazards. Transp. Res. A Policy Pract. 117, 214–226. https://doi.org/10.1016/j.tra.2018.08.030.

Loche, M., Alvioli, M., Marchesini, I., Bakka, H., Lombardo, L., 2022. Landslide susceptibility maps of Italy: lesson learnt from dealing with multiple landslide types and the uneven spatial distribution of the national inventory. Earth Sci. Rev. 232, 104125 https://doi.org/10.1016/j.earscirev.2022.104125.

Lorente, A., Beguería, S., Bathurst, J.C., García-Ruiz, J.M., 2003. Debris flow characteristics and relationships in the Central Spanish Pyrenees. Nat. Hazards Earth Syst. Sci. 3 (6), 683–691. https://doi.org/10.5194/nhess-3-683-2003.

Luo, H.Y., Zhang, L.M., Zhang, L.L., He, J., Yin, K.S., 2023. Vulnerability of buildings to landslides: the state of the art and future needs. Earth Sci. Rev. 238, 104329 https://doi.org/10.1016/j.earscirev.2023.104329.

Marchesini, I., Ardizzone, F., Alvioli, M., Rossi, M., Guzzetti, F., 2014. Non-susceptible landslide areas in Italy and in the Mediterranean region. Nat. Hazards Earth Syst. Sci. 14 (8), 2215–2231. https://doi.org/10.5194/nhess-14-2215-2014.

Marchesini, I., Rossi, M., Alvioli, M., Santangelo, M., Cardinali, M., 2020. Slope–catchment area relationship for debris-flow source area identification. In: Geomorphometry 2020. Sixth Geomorphometry Conference: Geomorphometry 2020, Perugia, Italy. https://doi.org/10.30437/geomorphometry2020_47.

Marchesini, I., Salvati, P., Rossi, M., Donnini, M., Sterlacchini, S., Guzzetti, F., 2021. Data-driven flood hazard zonation of Italy. J. Environ. Manag. 294, 112986 https://doi.org/10.1016/j.jenvman.2021.112986.

Marin, R.J., Velásquez, M.F., Sánchez, O., 2021. Applicability and performance of deterministic and probabilistic physically based landslide modeling in a data-scarce environment of the Colombian Andes. J. S. Am. Earth Sci. 108, 103175 https://doi.org/10.1016/j.jsames.2021.103175.

Martinović, K., Gavin, K., Reale, C., 2016. Development of a landslide susceptibility assessment for a rail network. Eng. Geol. 215, 1–9. https://doi.org/10.1016/j.enggeo.2016.10.011.

Mergili, M., Marchesini, I., Alvioli, M., Metz, M., Schneider-Muntau, B., Rossi, M., Guzzetti, F., 2014a. A strategy for GIS-based 3-D slope stability modelling over large areas. Geosci. Model Dev. 7 (6), 2969–2982. https://doi.org/10.5194/gmd-7-2969-2014.

Mergili, M., Marchesini, I., Rossi, M., Guzzetti, F., Fellin, W., 2014b. Spatially distributed three-dimensional slope stability modelling in a raster GIS. Geomorphology 206, 178–195. https://doi.org/10.1016/j.geomorph.2013.10.008.

Mergili, M., Krenn, J., Chu, H.-J., 2015. Randomwalk v1, a multi-functional conceptual tool for mass movement routing. Geosci. Model Dev. 8 (12), 4027–4043. https://doi.org/10.5194/gmd-8-4027-2015.

Mergili, M., Frank, B., Fischer, J.-T., Huggel, C., Pudasaini, S.P., 2018. Computational experiments on the 1962 and 1970 landslide events at Huascarán (Peru) with r.avaflow: Lessons learned for predictive mass flow simulations. Geomorphology 322, 15–28. https://doi.org/10.1016/j.geomorph.2018.08.032.

Mergili, M., Schwarz, L., Kociu, A., 2019. Combining release and runout in statistical landslide susceptibility modeling. Landslides 16 (11), 2151–2165. https://doi.org/10.1007/s10346-019-01222-7.

Palacio Cordoba, J., Mergili, M., Aristizábal, E., 2020. Probabilistic landslide susceptibility analysis in tropical mountainous terrain using the physically based r.slope.stability model. Nat. Hazards Earth Syst. Sci. 20 (3), 815–829. https://doi.org/10.5194/nhess-20-815-2020.

Park, H.J., Jang, J.Y., Lee, J.H., 2019. Assessment of rainfall-induced landslide susceptibility at the regional scale using a physically based model and fuzzy-based Monte Carlo simulation. Landslides 16 (4), 695–713. https://doi.org/10.1007/s10346-018-01125-z.

Petrova, E., Bostenaru Dan, M., 2020. Preface: Natural hazard impacts on technological systems and infrastructures. Nat. Hazards Earth Syst. Sci. 20 (10), 2627–2631. https://doi.org/10.5194/nhess-20-2627-2020.

Prochaska, A.B., Santi, P.M., Higgins, J.D., Cannon, S.H., 2008. Debris-flow runout predictions based on the average channel slope (ACS). Eng. Geol. 98 (1), 29–40. https://doi.org/10.1016/j.enggeo.2008.01.011.

Reichenbach, P., Rossi, M., Malamud, B.D., Mihir, M., Guzzetti, F., 2018. A review of statistically-based landslide susceptibility models. Earth Sci. Rev. 180, 60–91. https://doi.org/10.1016/j.earscirev.2018.03.001.

Rickenmann, D., 2005. Runout prediction methods. In: Jakob, M., Hungr, O. (Eds.), Debris-Flow Hazards and Related Phenomena. Springer, pp. 305–324. https://doi.org/10.1007/3-540-27129-5_13.

Rickenmann, D., Zimmermann, M., 1993. The 1987 debris flows in Switzerland: documentation and analysis. Geomorphology 8 (2), 175–189. https://doi.org/10.1016/0169-555X(93)90036-2.

Salvati, P., Petrucci, O., Rossi, M., Bianchi, C., Pasqua, A.A., Guzzetti, F., 2018. Gender, age and circumstances analysis of flood and landslide fatalities in Italy. Sci. Total Environ. 610–611, 867–879. https://doi.org/10.1016/j.scitotenv.2017.08.064.

Samela, C., Carisi, F., Domeneghetti, A., Petruccelli, N., Castellarin, A., Iacobini, F., Rinaldi, A., Zammuto, A., Brath, A., 2023. A methodological framework for flood hazard assessment for land transport infrastructures. Int. J. Disast. Risk Reduct. 85, 103491 https://doi.org/10.1016/j.ijdrr.2022.103491.

Santangelo, M., Marchesini, I., Bucci, F., Cardinali, M., Fiorucci, F., Guzzetti, F., 2015. An approach to reduce mapping errors in the production of landslide inventory maps. Nat. Hazards Earth Syst. Sci. 15 (9), 2111–2126. https://doi.org/10.5194/nhess-15-2111-2015.

Santangelo, M., Marchesini, I., Bucci, F., Cardinali, M., Cavalli, M., Crema, S., Marchi, L., Alvioli, M., Guzzetti, F., 2021. Exposure to landslides in rural areas in Central Italy. J. Maps 17 (4), 124–132. https://doi.org/10.1080/17445647.2020.1746699.

Schlögl, M., Matulla, C., 2018. Potential future exposure of European land transport infrastructure to rainfall-induced landslides throughout the 21st century. Nat. Hazards Earth Syst. Sci. 18 (4), 1121–1132. https://doi.org/10.5194/nhess-18-1121-2018.

Scotto di Santolo, A., Evangelista, A., 2009. Some observations on the prediction of the dynamic parameters of debris flows in pyroclastic deposits in the Campania region of Italy. Nat. Hazards 50 (3), 605–622. https://doi.org/10.1007/s11069-008-9334-3.

Steger, S., Brenning, A., Bell, R., Glade, T., 2017. The influence of systematically incomplete shallow landslide inventories on statistical susceptibility models and suggestions for improvements. Landslides 14 (5), 1767–1781. https://doi.org/10.1007/s10346-017-0820-0.

Steger, S., Scorpio, V., Comiti, F., Cavalli, M., 2022. Data-driven modelling of joint debris flow release susceptibility and connectivity. Earth Surf. Process. Landf. 47 (11), 2740–2764. https://doi.org/10.1002/esp.5421.

Tanyaş, H., Görüm, T., Kirschbaum, D., Lombardo, L., 2022. Could road constructions be more hazardous than an earthquake in terms of mass movement? Nat. Hazards 112 (1), 639–663. https://doi.org/10.1007/s11069-021-05199-2.

Tarquini, S., Nannipieri, L., 2017. The 10m-resolution TINITALY DEM as a trans-disciplinary basis for the analysis of the Italian territory: current trends and new perspectives. Geomorphology 281, 108–115. https://doi.org/10.1016/j.geomorph.2016.12.022.

Tarquini, S., Isola, I., Favalli, M., Mazzarini, F., Bisson, M., Pareschi, M.T., Boschi, E., 2007. TINITALY/01: a new triangular irregular network of Italy. Ann. Geophys. 50 (3), 407–425. https://doi.org/10.4401/ag-4424.

Taylor, F.E., Tarolli, P., Malamud, B.D., 2020. Preface: Landslide–transport network interactions. Nat. Hazards Earth Syst. Sci. 20 (10), 2585–2590. https://doi.org/10.5194/nhess-20-2585-2020.

Torri, D., Poesen, J., 2014. A review of topographic threshold conditions for gully head development in different environments. Earth Sci. Rev. 130, 73–85. https://doi.org/10.1016/j.earscirev.2013.12.006.

Trigila, A., Iadanza, C., Spizzichino, D., 2010. Quality assessment of the Italian Landslide Inventory using GIS processing. Landslides 7 (4), 455–470. https://doi.org/10.1007/s10346-010-0213-0.

Van den Bout, B., Tang, C., van Westen, C., Jetten, V., 2022. Physically based modeling of co-seismic landslide, debris flow, and flood cascade. Nat. Hazards Earth Syst. Sci. 22 (10), 3183–3209. https://doi.org/10.5194/nhess-22-3183-2022.

VanDine, D.F., 1985. Debris flows and debris torrents in the Southern Canadian Cordillera. Can. Geotech. J. 22 (1), 44–68. https://doi.org/10.1139/t85-006.

Voumard, J., Derron, M.-H., Jaboyedoff, M., 2018. Natural hazard events affecting transportation networks in Switzerland from 2012 to 2016. Nat. Hazards Earth Syst. Sci. 18 (8), 2093–2109. https://doi.org/10.5194/nhess-18-2093-2018.

Yin, L., Zhu, J., Li, W., Wang, J., 2022. Vulnerability analysis of geographical railway network under Geological Hazard in China. ISPRS Int. J. Geo Inf. 11 (6) https://doi.org/10.3390/ijgi11060342. Article 6.

Zhang, S., Zhang, L.-M., Chen, H.-X., Yuan, Q., Pan, H., 2013. Changes in runout distances of debris flows over time in the Wenchuan earthquake zone. J. Mt. Sci. 10 (2), 281–292. https://doi.org/10.1007/s11629-012-2506-y.

Zhao, J., Liu, K., Wang, M., 2020. Exposure analysis of Chinese railways to multihazards based on datasets from 2000 to 2016. Geomat. Nat. Haz. Risk 11 (1), 272–287. https://doi.org/10.1080/19475705.2020.1714753.